THE UNIVERSITY OF MICHIGAN

COLLEGE OF ENGINEERING

Department of Aerospace Engineering
High Altitude Engineering Laboratory

Scientific Report

ADMITTANCE OF THE INFINITE CYLINDRICAL ANTENNA IN A LOSSY PLASMA, II. THE INCOMPRESSIBLE, MAGNETOPLASMA

Edmund K. Miller

ORA Project 05627

under contract with:

NATIONAL AERONAUTICS AND SPACE ADMINISTRATION
CONTRACT NO. NASr-54(05)
WASHINGTON, D. C.

administered through:

OFFICE OF RESEARCH ADMINISTRATION ANN ARBOR

May 1967

TABLE OF CONTENTS

LIST OF FIGURES

Page

Abstract

Some numerical results are presented for the admittance of an infinite cylindrical antenna excited at a circumferential gap of finite thickness and immersed in a lossy, incompressible magnetoplasma, with the antenna axis parallel to the static magnetic field. The calculations are performed using a free-space layer of variable thickness (the vacuum sheath) to approximate the positive ion sheath which forms about a body at floating potential in a warm plasma. The antenna admittance is obtained by a direct numerical integration of the Fourier integral for the antenna current, and is presented for plasma parameter values typical of the E-region of the ionosphere.

The results obtained show that in the frequency range encompassing the electron plasma (f_p), electron cyclotron (f_h) and upper hybrid frequencies, the vacuum sheath considerably reduces variations in the admittance magnitude compared with the sheathless case. An admittance maximum which occurs at f_h for the sheathless case and which is more pronounced when $f_p > f_h$ than for the case where $f_p < f_h$, is reduced in amplitude and shifted upward in frequency by the vacuum sheath. The susceptance exhibits a slight minimum and the conductance a more pronounced minimum near f_p, when $f_p > f_h$, while for $f_p < f_h$, the conductance minimum is then less pronounced than the susceptance minimum, with the locations of these minima not appreciably different for the sheathless and vacuum sheath cases.

A comparison of these calculated results with some measurements of antenna impedance in the ionosphere, shows there to be a qualitative agreement between theory and experiment. In particular, an admittance minimum or discontinuity has be observed at the electron plasma frequency, similar to that seen in the calculated results, while an admittance maximum has been found above the electron cyclotron frequency, indicating the presence of a sheath.

I. Introduction

There is a great deal of interest today in the characteristics of antennas located in plasma media, such as the ionosphere, since a rocket or satellite-borne antenna may serve as a probe to determine the properties of the ambient ionosphere, such as electron plasma frequency, collision frequency and temperature. The present study has been undertaken in an attempt to gain a better understanding of the relative importance of the various factors which may influence the antenna admittance in the ionospheric plasma, such as acoustical and sheath effects which arise from the non-zero plasma temperature, and the ionospheric magnetic field. The antenna geometry chosen for the investigation is that of the infinite, cylindrical dipole driven at a circumferential gap of non-zero thickness, a geometry which allows a rigorous boundary value problem approach to be used. The case of the compressible (non-zero-temperature) magnetic-field-free plasma was reported on previously by the author (Miller, 1967a), which we refer to hereafter as I, and which is extended in the present report to the anisotropic plasma, there being a static magnetic field parallel to the infinite antenna axis. The present analysis will differ from I in that the electrokinetic (EK) electron pressure wave will not be included in the analysis, and it is in this sense, a zero temperature treatment. We will, as in I however, attempt to account for the positive ion sheath which forms about a body at floating potential in a non-zero temperature plasma. The plasma model thus used in that the plasma is of non-zero temperature insofar as its static behavior is concerned, but of zero temperature (imcompressible) in relation to its dynamic behavior.* While it would be desirable and more realistic to treat the compressible magnetoplasma, this is a generally very much more difficult problem than that discussed in I or to be considered here, and its treatment will be deferred to a subsequent report. A comparison of the theoretically determined results will be made with some experimental measurements of antenna impedance in the ionosphere. The RMKS system of units is used unless otherwise indicated, and equations referred to from I will be preceded by I.

---

*This means that the pressure term is set equal to zero in the time varying electron equation of motion.

II. Formulation

Our description of the plasma fields proceeds from the time dependent Maxwell's equations and the electron equation of motion, as

$$\nabla \times \underline{E}(\underline{r}, t) = -\mu_o \frac{\partial}{\partial t} \underline{H}(\underline{r}, t) \tag{1}$$

$$\nabla \times \underline{H}(\underline{r}, t) = \epsilon_o \frac{\partial}{\partial t} \underline{E}(\underline{r}, t) - N(\underline{r}, t)\underline{V}(\underline{r}, t)q \tag{2}$$

$$\left(\frac{\partial}{\partial t} + \underline{V}(\underline{r}, t)\cdot\nabla\right)\underline{V}(\underline{r}, t) = -\frac{q}{m}\underline{E}(\underline{r}, t) - \nu \underline{V}(\underline{r}, t)$$

$$-\frac{\nabla P(\underline{r}, t)}{mN(\underline{r}, t)} - \frac{q}{m}\mu_o \underline{V}(\underline{r}, t) \times \underline{H}(\underline{r}, t) \tag{3}$$

$$\left(\frac{\partial}{\partial t} + \underline{V}(\underline{r}, t)\cdot\nabla\right)N(\underline{r}, t) + N(\underline{r}, t)\nabla\cdot \underline{V}(\underline{r}, t) = 0 \tag{3a}$$

$$N(\underline{r}, t)\, T(\underline{r}, t)^{-1/(\gamma - 1)} = \text{constant} \tag{3b}$$

$$P(\underline{r}, t) = kN(\underline{r}, t)T(\underline{r}, t) \tag{3c}$$

where $\underline{E}$ and $\underline{H}$ are the total electric and magnetic fields, $\underline{V}$, N and P are the macroscopic electron velocity, number density, and pressure, T is the electron temperature, -q and m are the electron charge and mass, ν is the electron collision frequency, ϵ_o and μ_o are the permittivity and permeability of free space, k is Boltzmann's constant and $\underline{r}$ and t are the space and time coordinates. It should be noted here that while the pressure term in (3) has been indicated to be a function of both space and time coordinate, our treatment here will neglect the pressure term in (3). The equations (3a-3c) are included to show the full set required for the compressible plasma. The quantity γ is the ratio of specific heats for electron gas, and it may be seen from (3b) and (3c) that if $\gamma = 0$, then the dynamic pressure term is zero. This then is the implicit assumption in the following analysis for the unifrom plasma.

We deal with (1) - (3) in the usual way, introducing time varying or dynamic perturbation quantities small in comparison with the non-time varying or static quantities. Since the boundary value problem to be treated depends on the model used to represent the positive ion sheath, we will treat separately in turn in the following discussion the two sheath models to be used in the analysis. The first, or vacuum sheath model, replaces the actual sheath by a free space layer. In the second, or inhomogeneous sheath model, an attempt is made to include the actual sheath inhomogeneity in the analysis. In either case, the sheath forms a concentric layer between the antenna, located with its axis coincident with the z axis of the cylindrical coordinate system (ρ, φ, z) and the external uniform plasma, extending from $c \leq \rho \leq s$, where c and s are the cylinder and sheath-uniform plasma interface radii respectively. The antenna is excited by a circumferential gap of finite thickness δ across which a voltage V_o, independent of azimuthal coordinate φ, is applied. Contrary to the static magnetic-field-free case, azimuthal as well as z-directed currents are excited on the antenna. Our results will be primarily concerned with the z-component of current which determines the admittance, but some results will also be given for the φ-current component.

II. 1 The Vacuum Sheath

The merits and advantages of using the vacuum sheath model have been discussed in I, and so will not be considered further here. Equations (1) - (3) are linearized by introducing the following set of variables,

$$\underline{E}(\underline{r}, t) = \underline{e}(\underline{r}, t) \tag{4a}$$

$$\underline{H}(\underline{r}, t) = H\hat{z} + \underline{h}(\underline{r}, t) \; ; \quad |h| << |H| \tag{4b}$$

$$\underline{V}(\underline{r}, t) = \underline{v}(\underline{r}, t) \tag{4c}$$

$$N(\underline{r}, t) = N + n(\underline{r}, t) \; ; \; |n| << |N| \tag{4d}$$

$$T(\underline{r}, t) = T \tag{4e}$$

$$P(\underline{r}, t) = P \tag{4f}$$

The static externally applied magnetic field in the z-direction is H, and since the plasma is uniform, no static components of electric field or electron density are required. Upon introducing (4) into (1)-(3), we obtain

$$\nabla x \underline{e}(\underline{r}, t) = -\mu_o \frac{\partial}{\partial t} \underline{h}(\underline{r}, t) \tag{5}$$

$$\nabla x \underline{h}(\underline{r}, t) = \epsilon_o \frac{\partial}{\partial t} \underline{e}(r, t) - q N \underline{v}(\underline{r}, t) \tag{6}$$

$$\frac{\partial}{\partial t} \underline{v}(\underline{r}, t) = -\frac{q}{m} \underline{e}(\underline{r}, t) - \nu \underline{v}(\underline{r}, t) - \frac{q}{m} \mu_o H \underline{v}(\underline{r}, t) x \hat{z} \tag{7}$$

If we use the Fourier transform pair

$$\underline{e}(\underline{r}, t) = \frac{1}{2\pi} \int_{-\infty}^{\infty} e^{i\omega t} \tilde{\underline{e}}(\underline{r}, \omega) \, d\omega$$

$$\tilde{\underline{e}}(\underline{r}, \omega) = \int_{-\infty}^{\infty} e^{-i\omega t} \underline{e}(\underline{r}, t) \, dt$$

then (5) - (7) becomes

$$\nabla x \tilde{\underline{e}}(\underline{r}, \omega) = -i\omega\mu_o \tilde{\underline{h}}(\underline{r}, \omega) \tag{8}$$

$$\nabla x \tilde{\underline{h}}(\underline{r}, \omega) = i\omega \epsilon_o \tilde{\underline{e}}(\underline{r}, \omega) - q N \tilde{\underline{v}}(\underline{r}, \omega) \tag{9}$$

$$(i\omega + \nu) \tilde{\underline{v}}(\underline{r}, \omega) = -\frac{q}{m} \left[\tilde{\underline{e}}(\underline{r}, \omega) + \mu_o H \tilde{\underline{v}}(\underline{r}, \omega) x \hat{z} \right] \tag{10}$$

We may solve for $\tilde{\underline{v}}(\underline{r}, \omega)$ from (10) to get

$$\tilde{v}_z = -\frac{q}{i\omega' m} \tilde{e}_z \tag{11a}$$

$$\tilde{v}_\varphi = -\frac{\epsilon_o \omega_p^2}{i\omega' q}\left[\tilde{e}_\varphi + \frac{\omega_h}{i\omega'} \tilde{e}_\rho\right]\left[1 - (\omega_h/\omega')^2\right]^{-1} \tag{11b}$$

$$\tilde{v}_\rho = -\frac{\epsilon_o \omega_p^2}{i\omega' q}\left[\tilde{e}_\rho - \frac{\omega_h}{i\omega'} \tilde{e}_\varphi\right]\left[1 - (\omega_h/\omega')^2\right]^{-1} \tag{11c}$$

where

$$\omega_p^2 = \frac{q^2 N}{\epsilon_o m} = (2\pi f_p)^2$$

$$\omega_h = \frac{q\mu_o H_o}{m}$$

$$\omega' = \omega\,(1 + \nu/i\,\omega)$$

Equation (9) can then be written

$$\nabla \times \tilde{\underline{h}} = i\omega \epsilon_o \underline{\underline{\epsilon}} \cdot \tilde{\underline{e}} \tag{9a}$$

where

$$\underline{\underline{\epsilon}} = \begin{bmatrix} \epsilon_1 & \epsilon' & 0 \\ -\epsilon' & \epsilon_1 & 0 \\ 0 & 0 & \epsilon_3 \end{bmatrix} \tag{12a}$$

and

$$\epsilon_1 = 1 - \frac{\omega_p^2}{\omega\,\omega'} \frac{1}{(1-\omega_h^2/\omega'^2)} \tag{12b}$$

$$\epsilon_3 = 1 - \frac{\omega_p^2}{\omega\,\omega'} \tag{12c}$$

$$\epsilon' = \frac{\omega_p \omega_h}{i\omega\omega'^2} \frac{1}{(1-\omega_h^2/\omega'^2)} \tag{12d}$$

The component equations of (8) and (9) are then obtained by introducing a second Fourier transform pair

$$\underline{\tilde{\tilde{e}}}(\rho,\beta,\omega) = \int_{-\infty}^{\infty} e^{-i\beta z}\, \underline{\tilde{e}}(\underline{r},\omega)\, dz$$

$$\underline{\tilde{e}}(\underline{r},\omega) = \frac{1}{2\pi}\int_{-\infty}^{\infty} e^{+i\beta z}\, \underline{\tilde{\tilde{e}}}(\rho,\beta,\omega)\, d\beta$$

and are found to be

$$-i\beta\, \tilde{\tilde{e}}_{\varphi} = -i\omega\mu_o \tilde{\tilde{h}}_{\rho} \tag{13a}$$

$$i\beta\, \tilde{\tilde{e}}_{\rho} - \tilde{\tilde{e}}_z' = i\omega\mu_o \tilde{\tilde{h}}_{\varphi} \tag{13b}$$

$$\tilde{\tilde{e}}_{\varphi}' + \tilde{\tilde{e}}_{\varphi}/\rho = -i\omega\mu_o \tilde{\tilde{h}}_z \tag{13c}$$

$$-i\beta \tilde{\tilde{h}}_{\varphi} = i\omega\epsilon_o(\epsilon_1 \tilde{\tilde{e}}_{\rho} + \epsilon' \tilde{\tilde{e}}_{\varphi}) \tag{14a}$$

$$i\beta\, \tilde{\tilde{h}}_{\rho} - \tilde{\tilde{h}}_z' = i\omega\epsilon_o(\epsilon_1 \tilde{\tilde{e}}_{\varphi} - \epsilon' \tilde{\tilde{e}}_{\rho}) \tag{14b}$$

$$\tilde{\tilde{h}}_{\varphi}' + \tilde{\tilde{h}}_{\varphi}/\rho = i\omega\epsilon_o \epsilon_3 \tilde{\tilde{e}}_z \tag{14c}$$

where the prime indicates differentiation with respect to ρ. Note that the fields are independent of the aziumthal coordinate.

We may obtain expression for the ρ and φ field components in terms of the z components, which are

$$\tilde{\tilde{e}}_{\rho} = -i(\beta A \tilde{\tilde{e}}_z' + \omega\mu_o B \tilde{\tilde{h}}_z')/D \tag{15a}$$

$$\tilde{\tilde{e}}_{\varphi} = i(\beta B \tilde{\tilde{e}}_z' - \omega\mu_o A \tilde{\tilde{h}}_z')/D \tag{15b}$$

$$\tilde{\tilde{h}}_{\rho} = \beta\, \tilde{\tilde{e}}_{\varphi}/\omega\mu_o \tag{16a}$$

$$\tilde{\tilde{h}}_{\varphi} = i\omega\epsilon_o(\epsilon_1 A - \epsilon' B)\, \tilde{\tilde{e}}_z'/D + i\beta B\, \tilde{\tilde{h}}_z'/D \tag{16b}$$

$$A = \beta^2 - K_{Eo}^2 \epsilon_1$$

$$B = K_{Eo}^2 \epsilon'$$

$$D = A^2 + B^2$$

$$K_{Eo}^2 = \omega^2 \mu_o \epsilon_o$$

Finally, two coupled scalar wave equations for the z-components of the field are obtained,

$$\left(\underline{\underline{C}} \nabla_\rho^2 + \underline{\underline{Z}} \right) \begin{bmatrix} \tilde{\tilde{e}}_z \\ \tilde{\tilde{h}}_z \end{bmatrix} = 0 \tag{17}$$

with

$$\underline{\underline{C}} = \begin{bmatrix} 1 - \beta^2 A/D & -\beta\omega\mu_o B/D \\ \beta\omega\epsilon_o\epsilon' A/D & 1 - K_{Eo}^2 \epsilon' B/D \end{bmatrix} \tag{18a}$$

$$\underline{\underline{Z}} = \begin{bmatrix} K_{Eo}^2 \epsilon_3 & O \\ O & -A \end{bmatrix} \tag{18b}$$

We note that when the static magnetic field is made zero, then B and ϵ' become zero, and (17) decouples. The equations are decoupled by a standard technique when there is a non-zero magnetic field. First we let

$$\begin{bmatrix} \tilde{\tilde{e}}_z \\ \tilde{\tilde{h}}_z \end{bmatrix} = \begin{bmatrix} T_{11} & T_{12} \\ T_{21} & T_{22} \end{bmatrix} \begin{bmatrix} G_1 \\ G_2 \end{bmatrix} \tag{19}$$

so that (17) may be written

$$(\underline{\underline{C}} \nabla_\rho^2 + \underline{\underline{Z}})\ \underline{\underline{T}}\ \underline{G} = O \tag{20}$$

Multiplying from the left by $\underline{\underline{C}}^{-1}$ and then by $\underline{\underline{T}}^{-1}$ yields

$$\nabla_\rho^2 \underline{G} + \underline{\underline{T}}^{-1} \underline{\underline{C}}^{-1} \underline{\underline{Z}} \underline{\underline{T}} \underline{G} = O \tag{21}$$

where

$$\underline{\underline{C}}^{-1}\underline{\underline{Z}} = \begin{bmatrix} (K_{Eo}^2 - \beta^2/\epsilon_1)\epsilon_3 \; ; \; \beta\omega\mu_o\epsilon'/\epsilon_1 \\ -\beta\omega\epsilon_o\epsilon_3\epsilon'/\epsilon_1 \; ; \; K_{Eo}^2(\epsilon_1 + \epsilon'^2/\epsilon_1) - \beta^2 \end{bmatrix}$$

If $\underline{\underline{T}}$ is so chosen as to diagonalize the $\underline{\underline{C}}^{-1}\underline{\underline{Z}}$ term in (21), then the equations are coupled, and

$$\nabla^2 G_j + \lambda_j G_j = 0; j = 1, 2 \qquad (22)$$

where the λ_j, the eigen values of the matrix

$$\underline{\underline{C}}' = \underline{\underline{C}}^{-1}\underline{\underline{Z}}$$

are solutions of

$$\underline{\underline{C}}'\underline{T}_j = \lambda_j \underline{T}_j \quad ; j = 1, 2 \qquad (23)$$

where $\underline{T}_j$ is an eigen vector of $\underline{\underline{C}}'$. Solving for λ_j from

$$|\underline{\underline{C}}' - \lambda_j \underline{\underline{I}}| = 0 \qquad (24)$$

where the $|\ |$ denotes the determinant of the enclosed matrix and $\underline{\underline{I}}$ is the identity matrix, we obtain

$$\lambda_j = \left[(C'_{11} + C'_{22}) \pm \sqrt{(C'_{11} + C'_{22})^2 - 4\,|\underline{\underline{C}}'|} \right] / 2; \qquad (25)$$

The eigen vector elements are found from (23)

$$T_{12} = T_{22} C'_{12} / (\lambda_2 - C'_{11}) \qquad (26a)$$

$$T_{21} = T_{11} C'_{21} / (\lambda_1 - C'_{22}) \qquad (26b)$$

Since there are two equations for determining the four eigen vector elements T_{ij}, two of them may be chosen arbitrarily,

and for convenience we set $T_{11} = T_{22} = 1$ in the following.

The solutions of (22) with which we are concerned are simply given by

$$G_j = A_j H_o^{(2)} (\sqrt{\lambda_j}\rho) \tag{27}$$

since (22) applies to the uniform plasma outside the vacuum sheath where there is one outward traveling wave of amplitude A_j for each G_j. The A_j are of course determined by the boundary conditions. One precaution must be mentioned here and that is that the G_j must be well-behaved at infinity. Consequently, the sign of the imaginary part of the Hankel function argument in (27) must be always negative, which specifies the sign of the root of λ_j. Other ways of choosing the proper solutions for G_j have been discussed by Seshadri and Wu (1966), which involve time casuality and require changing the Hankel function kind rather than the root sign of λ_j to acheive the same end. In the numerical approach to be taken here, the former approach is straight forward and perhaps simpler to apply, and for this reason has been used in obtaining our numerical results.

The electric fields in the vacuum sheath are easily obtained from scalar potential functions as

$$\underset{\sim}{\tilde{e}}_e = \nabla \times (\tilde{\phi}_e \hat{z}) \tag{28a}$$

$$\underset{\sim}{\tilde{e}}_m = \frac{1}{K_{Eo}} \nabla \times \nabla \times (\tilde{\phi}_m \hat{z}) \tag{28b}$$

where the e and m subscripts denote the transverse electric (TE) (e_z=0) and transverse nagnetic (TM) (h_z=0) polarizations, and the magnetic fields are found from (13). The potential functions are solution to

$$(\nabla_\rho^2 + K_{Eo}^2)\tilde{\phi}_{e,m} = 0 \tag{29}$$

and are

$$\tilde{\phi}_{e,m} = A^I_{e,m} H_o^{(2)} (\lambda_{Eo}\rho) + A^R_{e,m} H_o^{(1)} (\lambda_{Eo}\rho) \tag{30}$$

where

$$\lambda_{Eo}^2 = K_{Eo}^2 - \beta^2$$

and the superscripts I and R denote respectively the fields incident on the sheath-plasma interface from the antenna, and those reflected back towards the antenna with the wave amplitudes given by A.

The specification of the problem is completed by giving the boundary conditions which the fields must satisfy at the antenna surface and the sheath-plasma interface. Six scalar boundary conditions are necessary since there are six wave amplitudes, or spectral Fourier coefficients, which are functions of β and ω, to be determined. The continuity of the tangential electric and magnetic fields at the sheath-plasma interface, and the vanishing of the φ -component of electric field on the antenna surface produces five of the required six equations.

The final boundary condition is a function of the exciting source, in this case a circumferential gap of thickness δ, centered at z=0. A voltage $V_o(t)$ which is independent of azimuthal angle φ, is applied across the gap, so that

$$-V_o(t) = \int_{-\delta/2}^{\delta/2} e_z(c, z, t)\,dz \qquad (31)$$

since e_z is zero for $|z| > \delta/2$. If $\delta \ll K_{Eo}^{-1}$ and $\delta \ll 2c$, where c is the antenna radius, then e_z is practically uniform across the gap, and

$$\begin{aligned} e_z(c, z, t) &= -V_o(t)/\delta \quad ; \quad |z| < \delta/2 \\ &= 0 \quad ; \quad |z| > \delta/2 \end{aligned} \qquad (32)$$

If the source is nonchromatic, i.e.

$$V_o(t) = V_o e^{i\omega t}$$

then

$$\tilde{e}_z(c, z, \omega) = -V_o\, \delta(\omega-\omega')\, 2\pi/\delta \qquad (33)$$

where $\delta(\omega-\omega')$ is the delta function, and

$$\begin{aligned} \tilde{\tilde{e}}_z(c, \beta, \omega) &= -V_o\, \delta(\omega-\omega')\, \frac{\sin(\beta\delta/2)}{(\beta\delta/2)}\, 2\pi \\ &= S(\beta) V_o\, \delta(\omega-\omega')\, 2\pi \\ &= \bar{S}(\beta) \end{aligned} \qquad (34)$$

Upon using (28), (30) and (34), the boundary conditions on the antenna may be written as

$$\frac{\lambda_{Eo}^2}{K_{Eo}} \left[A_m^I \; H_o^{(2)} (\lambda_{Eo} c) + A_m^R H_o^{(1)} (\lambda_{Eo} c) \right] = \bar{S}(\beta) \qquad (35a)$$

$$A_e^I \; H_o^{(2)'} (\lambda_{Eo} c) + A_e^R H_o^{(1)'} (\lambda_{Eo} c) = 0 \qquad (35b)$$

where the prime now denotes differentiation with respect to argument. In a similar fashion, the boundary conditions at the sheath-plasma interface (ρ=s) are

$$\frac{\lambda_{Eo}^2}{K_{Eo}} \left[A_m^I \; H_o^{(2)} (\lambda_{Eo} s) + A_m^R \; H_o^{(1)} (\lambda_{Eo} s) \right] = \approx{e}_z \qquad (36a)$$

$$-\lambda_{Eo} \left[A_e^I \; H_o^{(2)'} (\lambda_{Eo} s) + A_e^R \; H_o^{(1)'} (\lambda_{Eo} s) \right] = \approx{e}_\varphi \qquad (36b)$$

$$\frac{i \; \lambda_{Eo}^2}{\eta_o K_{Eo}} \left[A_e^I \; H_o^{(2)} (\lambda_{Eo} s) + A_e^R \; H_o^{(1)} (\lambda_{Eo} s) \right] = \approx{h}_z \qquad (36c)$$

$$-\frac{i \; \lambda_{Eo}}{\eta_o} \left[A_m^I \; H_o^{(2)'} (\lambda_{Eo} s) + A_m^R \; H_o^{(1)'} (\lambda_{Eo} s) \right] = \approx{h}_\varphi \qquad (36d)$$

where the quantities on the righthand side of (36) are the plasma fields evaluated at ρ=s.

The 6 x 6 matrix represented by (35) and (36) may be reduced, by the use of (15), (16), (19) and (27), to the following system of equations, with the prime denoting differentiation with respect to argument,

$$\begin{bmatrix} & & & & & \\ & & \triangle & & & \\ & & & & & \end{bmatrix} \begin{bmatrix} \bar{A}_m^I \\ \bar{A}_e^I \\ \bar{A}_1 \\ \bar{A}_2 \end{bmatrix} = \begin{bmatrix} S_1 \\ 0 \\ 0 \\ S_2 \end{bmatrix} \qquad (37)$$

with $A_{\_} = V_o \, \delta(\omega-\omega') \; 2\pi \; S(\beta) \; \bar{A}_{\_}$

and where

$$S_1 = \frac{H_{1s}}{H_{1c}} \tag{38a}$$

$$S_2 = \frac{iK_{Eo}}{\eta_o \lambda_{Eo}} \frac{H'_{1s}}{H_{1c}} \tag{38b}$$

$$[\triangle] = \begin{bmatrix} -\frac{\lambda^2_{Eo}}{K_{Eo}} \frac{W(c,s)}{H_{1c}} ; & 0; & H_1; & T_{12} H_2 \\ 0 & ; \lambda_{Eo} \frac{W(c',s')}{H'_{1c}} & ; C_1 H'_1 ; & C_2 H'_2 \\ 0 & ; -\frac{i\lambda^2_{Eo} W(c',s)}{\eta_o K_{Eo} H'_{1c}} & ; T_{21} H_1; & H_2 \\ \frac{i\lambda_{Eo} W(c,s')}{\eta_o H_{1c}} & ; 0 & ; C_3 H'_1 ; & C_4 H'_2 \end{bmatrix} \tag{38c}$$

$$H_{nx} = H_o^{(n)} (\lambda_{Eo} x) \tag{39a}$$

$$H_n = H_o^{(2)} (\sqrt{\lambda}_n s) \tag{39b}$$

$$W(c,s) = H_{1c} H_{2s} - H_{1s} H_{2c} \tag{40a}$$

$$W(c',s) = H'_{1c} H_{2s} - H_{1s} H'_{2c} \tag{40b}$$

$$W(c,s') = H_{1c} H'_{2s} - H'_{1s} H_{2c} \tag{40c}$$

$$W(c',s') = H'_{1c} H'_{2s} - H'_{1s} H'_{2s} \tag{40d}$$

$$C_1 = i\sqrt{\lambda_1} (\beta B - \omega\mu_o A T_{21}) / D$$

$$C_2 = i\sqrt{\lambda_2} (\beta B T_{12} - \omega\mu_o A) / D$$

$$C_3 = i\sqrt{\lambda_1} [\omega\epsilon_o \epsilon_1 A + B(\beta T_{21} - \omega\epsilon_o \epsilon')] / D$$

$$C_4 = i\sqrt{\lambda_2} [\omega\epsilon_o \epsilon_1 A T_{12} + B(\beta - \omega\epsilon_o \epsilon' T_{12})] / D$$

Note that, in the plasma

$$\tilde{\tilde{h}}_\varphi = C_3 A_1 H_1' + C_4 A_2 H_2' \tag{41a}$$

$$\tilde{\tilde{e}}_\varphi = C_1 A_1 H_1' + C_2 A_2 H_2' \tag{41b}$$

$$\tilde{\tilde{e}}_z = A_1 H_1 + T_{12} A_2 H_2 \tag{41c}$$

$$\tilde{\tilde{h}}_z = T_{21} A_1 H_1 + A_2 H_2 \tag{41d}$$

where the s in (39b) is replaced by ρ, while in the sheath

$$\tilde{\tilde{h}}_\varphi = C_3' \tilde{\tilde{e}}_z' + C_4' \tilde{\tilde{h}}_z' \tag{41e}$$

$$\tilde{\tilde{e}}_\varphi = C_1' \tilde{\tilde{e}}_z' + C_2' \tilde{\tilde{h}}_z' \tag{41f}$$

where $C_1' = C_1 \sqrt{\lambda_1}$; $C_3' = C_3 \sqrt{\lambda_3}$

$C_2' = C_2 \sqrt{\lambda_2}$; $C_4' = C_4 \sqrt{\lambda_4}$

with $T_{12} = T_{21} = 0$

and ω_p is set equal to 0.

We may finally obtain the current on the antenna as

$$I_z(z,t) = 2\pi c h_\varphi(z,t)$$

$$= \frac{-icV_o}{\eta_o} \iint_{-\infty}^{\infty} e^{i(\omega' t + \beta z)} \delta(\omega-\omega') \left[\frac{K_{Eo}}{\lambda_{Eo}} H_o^{(2)'}(\lambda_{Eo} c) + \frac{4i}{\pi c} \bar{A}_m^R \right] \frac{S(\beta)}{H_o^{(2)}(\lambda_{Eo} c)} \, d\beta \, d\omega'$$

$$= \frac{-icV_o e^{i\omega t}}{\eta_o} \int_{-\infty}^{\infty} \frac{e^{i\beta z} S(\beta)}{H_o^{(2)}(\lambda_{Eo} c)} \left[\frac{K_{Eo}}{\lambda_{Eo}} H_o^{(2)'}(\lambda_{Eo} c) + \frac{4i}{\pi c} \bar{A}_m^R \right] d\beta$$

$$= I_z(z,\omega) \, e^{i\omega t} \tag{42}$$

$$I_\varphi(z,t) = -2\pi c h_z(z,t)$$

$$= \frac{4V_o}{\eta_o K_{Eo} \pi} \int\int_{-\infty}^{\infty} e^{i(\omega' t + \beta z)} \delta(\omega - \omega') \frac{\bar{A}_e^R S(\beta) d\omega' d\beta}{H_o^{(2)'}(\lambda_{Eo} c)}$$

$$= \frac{4V_o e^{i\omega t}}{\eta_o K_{Eo} \pi} \int_{-\infty}^{\infty} e^{i\beta z} \frac{\bar{A}_e^R S(\beta) d\beta}{H_o^{(2)'}(\lambda_{Eo} c)} \tag{43}$$

$$= I_\varphi(z,\omega)\, e^{i\omega t} = 2\pi c K_\varphi(z,\omega)\, e^{i\omega t}$$

Note that K_φ is the φ -component of current density, but that we will present the quantity I_φ in order to make a direct comparison with I_z.

We see that I_z contains two terms, the first being that for the free space current on the infinite antenna and the second term, which contains $\bar{A}_m^R$, showing the perturbing influence of the plasma on the antenna current. Thus, with I_{zo} the free space current,

$$I_z(z,\omega) - I_{zo}(z,\omega) = \Delta I_z(z,\omega)$$

where

$$I_{zo}(z,\omega) = -\frac{icK_{Eo}V_o}{\eta_o} \int_{-\infty}^{\infty} \frac{e^{i\beta z} H_o^{(2)'}(\lambda_{Eo} c)}{\lambda_{Eo}\, H_o^{(2)}(\lambda_{Eo} c)} S(\beta) d\beta \tag{44}$$

$$\Delta I_z(z,\omega) = \frac{4V_o}{\eta_o \pi} \int_{-\infty}^{\infty} \frac{e^{i\beta z}}{H_o^{(2)}(\lambda_{Eo} c)} S(\beta) \bar{A}_m^R\, d\beta \tag{45}$$

The numerical evaluation of $I_{zo}(z,\omega)$ has been carried out by Duncan (1962), and Einarson (1966) while approximate analytic expressions have been derived by Chen and Keller (1962) and Fante (1966). A discussion of both aspects of this problem is given by Miller (1967b). Note that the limits of integration of (42) - (45) may be transformed to the range zero to infinity because the integrand functions are even in β, and the exponential function then becomes $\cos(\beta z)$.

An important point to consider in evaluating (44) is that there is an integrable singularity at $\beta = K_{Eo}$ in the real part of the integral, but non-integrable singularities on either side of $\beta = K_{Eo}$ in the imaginary part. The real component of free space current is thus more readily obtained than the imaginary part, since in addition, the real component comes entirely from the finite range $\beta = 0$ to K_{Eo} while the imaginary component comes from the entire range of β. When the entire integrand appearing in (42) is examined however, it may be shown that the non-integrable singularities cancel, with the result that the integration contour can follow the real β-axis. The evaluation of (43) also follows in the same way. The details are shown in Appendix A.

The numerical problem of solving (42) and (43) is, while formally straightforward, quite complicated because of the nature of the integrand functions. These integrand functions vary over a wide range in magnitude, and are very rapidly changing in the vicinity of their near singularities with the result that the abscissa spacing used for the summing process must be adjusted accordingly. An integration program using a variable integration interval width, and making use of the Romberg integration technique was developed for this purpose. The details are given by Miller (1967a); the main feature of this method is that the Romberg technique provides a convergence test which allows the integration to be performed maintaining a desired accuracy within each finite-width interval of the β variation, while at the same time nearly optimizing the number of abscissa points required for this desired accuracy.

The antenna admittance is finally obtained from

$$Y(\omega) = \frac{I_z(\delta/2, \omega)}{V_o} = G(\omega) + iB(\omega) \qquad (46)$$

where G is the conductance and B the susceptance. Note that B is finite only for a non-zero exciting gap thickness, while G is not generally sensitive to the gap thickness, at least for small gaps. Further discussion of this question is given by Miller (1967b).

It should be noted that for the results to be presented, only (42), evaluated at $z = \delta/2$, was subjected to the convergence test used for the numerical integration. This was done to minimize the computer time required (which was about 1 minute/admittance value on an IBM 7090 computer) to obtain the admittance values, the quantities of primary interest in this study. Since the integrand of (43) may require a different sequence of abscissa spacings for a prescribed summation accuracy than (42), this means that the values obtained for I_φ may not have the same accuracy as the corresponding $I_z(\delta/2, \omega)$. This same observation applies to (42) evaluated for values of z other than $\delta/2$, the value of z used for the convergence test.

It is felt that the convergence errors associated with replacing the integration process by a summation are no larger than 1 or 2 units in the third significant figure in the admittance. Another factor in determining the final accuracy is the truncation error resulting from terminating the infinite integration range at a finite β value. The largest β value that could be used generally was determined by overflow in the computer, i.e., numbers too large for the computer were obtained. The real component of current for the plasma medium, as for free space mentioned above, is convergent on a finite β-range, generally well before any overflow problems are encountered. The imaginary component on the other hand requires a considerably greater β-range in order to be determined to the same accuracy as the real

component, but it may happen that overflow occurs before this range is entirely integrated, with a resultant decrease in the relative accuracy of the imaginary component. In addition, the imaginary component may also change in sign as β is increasing, so that the error resulting from too-early truncation of the integration because of overflow may be relatively much larger. The overall accuracy of the conductance is estimated to be no less than 0.1 percent. The susceptance may be less well determined, and in presenting the results, those areas where the susceptance is estimated to be known to no better than 10 percent accuracy will be denoted. (A discussion or the truncation error resulting when the β-range is not limited by overflow is given by Miller (1967a)).

II. 2 The Inhomogeneous Sheath

The inhomogeneous sheath boundry value problem differs from that of the vacuum sheath discussed above in only the sheath of course, since the fields in the external uniform plasma are described by the same equations. Consequently, the discussion here is concerned only with the sheath. The uniform plasma equations apply in the sheath, with the exception that now (4a) and (4d) are replaced by

$$\underline{E}\ (\underline{r},\ t) = \underline{E}\ (\underline{r}) + \underline{e}\ (\underline{r},\ t)\ ; \quad |e| << |E| \tag{4a)'}$$

$$N\ (\underline{r},\ t) = N\ (\underline{r}) + n\ (\underline{r},\ t)\ ; \quad |n| << |N| \tag{4d)'}$$

$$P\ (\underline{r},\ t) = P\ (\underline{r}) = k\ T\ N\ (\underline{r}) \tag{4f)'}$$

We note that there is a static component of electric field in the sheath, but since the EK wave is not considered in this analysis, its effect on the EM wave is an indirect one produced by the resulting inhomogeneity in the electron density in the sheath.

The static protions of (1-3) are now

$$\nabla \times \underline{E}\ (\underline{r}) = 0 \tag{47}$$

$$q\ \underline{E}\ (\underline{r}) + \frac{k\ T\ \nabla N\ (r)}{N\ (\underline{r})} = 0 \tag{48}$$

Since then from (47)

$$\underline{E} = -\nabla \phi$$

and $$N\ (\underline{r}) = N_{\infty}\ \exp\left[\ q\ \phi(\underline{r})/k\ T\right] \tag{49a}$$

with N_{∞} the electron density in the uniform plasma. The dynamic equations are unchanged from those which apply in the uniform plasma except that now N is replaced by N $(\underline{r})$.

The static sheath potential ϕ is taken as

$$\phi = \phi_c \left[\frac{s-\rho}{s-c}\right]^M \tag{49b}$$

with M an adjustable parameter and ϕ_c the cylinder potential,

$$\phi_c = - \frac{k\ T}{q} \left[\ln \left(\sqrt{\frac{m_i}{m}} \quad \frac{1}{1.22} \right) \right] \tag{49c}$$

where m_i is the ion mass and k is Boltzmann's constant. A more complete discussion of this form for the potential is given by Miller (1966a).

The analysis follows that in the preceding section, through Eq. (16). The wave equations corresponding to (17) however now have additional terms involving the first derivative of the field components and cannot be decoupled in the same way. It thus becomes preferable to deal numerically with the first order differential equations (13) and (14) in the sheath and match these to the analytic solutions obtainable in the uniform plasma at the sheath-uniform plasma interface. We thus solve

$$\approx{e}_z' = i\beta \approx{e}_\rho + i\omega\mu_o \approx{h}_\varphi \tag{50a}$$

$$\approx{e}_\varphi' = - \approx{e}_\varphi / \rho - i\omega\mu_o \approx{h}_z \tag{50b}$$

$$\approx{h}_z' = - i\omega\epsilon_o (\epsilon_1 \approx{e}_\varphi - \epsilon' \approx{e}_\rho) + i\beta \approx{h}_\rho \tag{50c}$$

$$\approx{h}_\varphi' = i\omega\epsilon_o\epsilon_3 \approx{e}_z - \approx{h}_\varphi / \rho \tag{50d}$$

where $$\approx{e}_\rho = \frac{-1}{i\omega\epsilon_o\epsilon_1} (i\omega\epsilon_o\epsilon' \approx{e}_\varphi + i\beta \approx{h}_\varphi) \tag{50e}$$

and $$\approx{h}_\rho = \beta \approx{e}_\varphi / \omega\mu_o \tag{50f}$$

subject to the boundary condition that at $\rho = c$:

$$\approx{e}_\varphi = 0 \tag{51a}$$

$$\approx{e}_z = - S(\beta)\ V_o\ \delta(\omega-\omega')\ 2\pi \tag{51b}$$

and at $\rho = s$:

$$\tilde{\tilde{e}}_\varphi \Big|_{\text{sheath}} = \tilde{\tilde{e}}_\varphi \Big|_{\text{plasma}} \tag{52a}$$

$$\tilde{\tilde{e}} \Big|_{\text{sheath}} = \tilde{\tilde{e}}_z \Big|_{\text{plasma}} \tag{52b}$$

$$\tilde{\tilde{h}}_\varphi \Big|_{\text{sheath}} = \tilde{\tilde{h}}_\varphi \Big|_{\text{plasma}} \tag{52c}$$

$$\tilde{\tilde{h}}_z \Big|_{\text{sheath}} = \tilde{\tilde{h}}_z \Big|_{\text{plasma}} \tag{52d}$$

The plasma fields may be written explicitely in terms of the Fourier coefficients for the transmitted fields, as in eq. (42), and upon eliminating the Fourier coefficients from the boundary conditions (52) we obtain at $\rho = s$, with $T' = |\underline{\underline{T}}|$

$$C_1 \tilde{\tilde{e}}_z' + C_2 \tilde{\tilde{h}}_z' = C_1 H_1' (\tilde{\tilde{e}}_z - T_{12} \tilde{\tilde{h}}_z) / H_1 T' - C_2 H_2' (\tilde{\tilde{e}}_z T_{21} - \tilde{\tilde{h}}_z) / H_2 T' \tag{53a}$$

$$C_3 \tilde{\tilde{e}}_z' + C_4 \tilde{\tilde{h}}_z' = C_3 H_1' (\tilde{\tilde{e}}_z - T_{12} \tilde{\tilde{h}}_z) / H_1 T' - C_4 H_2' (\tilde{\tilde{e}}_z T_{21} - \tilde{\tilde{h}}_z) / H_2 T' \tag{53b}$$

The fourth order differential equation (50) together with the four boundary conditions (51) and (53) thus describe the problem of the inhomogeneous sheath. Note that all quantities involving the electron density are, in the sheath, functions of the radial variable.

The antenna current is obtained, as before, from the magnetic field on the cylinder surface, and is

$$\begin{aligned} I_z(z,t) &= 2\pi c h_\varphi (c,z,t) \\ &= \frac{c}{2\pi} \int_{-\infty}^{\infty}\int e^{i(\omega' t + \beta z)} \tilde{\tilde{h}}_\varphi (c,\beta,\omega')\, d\beta\, d\omega' \\ &= c\, e^{i\omega t} \int_{-\infty}^{\infty} e^{i\beta z} \bar{h}_\varphi (c,\beta)\, d\beta \\ &= I_z(z,\omega)\, e^{i\omega t} \end{aligned} \tag{54a}$$

$$I_{\varphi}(z,t) = -2\pi c h_z(c,z,t)$$

$$= \frac{-c}{2\pi} \iint_{-\infty}^{\infty} e^{i(\omega' t + \beta z)} \approx{h}_z(c,\beta,\omega')\, d\beta\, d\omega'$$

$$= c\, e^{i\omega t} \int_{-\infty}^{\infty} e^{i z} \bar{h}_z(c,\beta,\omega)\, d\beta$$

$$= I(z,\omega)\, e^{i\omega t} \qquad (54b)$$

where $\approx{h}_-(c,\beta,\omega) = V_o S(\beta)\ \delta(\omega-\omega')\, 2\pi\ \bar{h}_-(c,\beta,\omega)$

The technique of solving such a two point boundary value problem is discussed in detail by Miller (1966b). It involves in the present problem, two numerical integrations, one to solve the differential equations and the other to perform the integration over β . Consequently, this is a very time consuming calculation, and for this report, numerical results are to be presented for only the vacuum sheath model.

III. Numerical Results

III. 1. The Infinite Antenna Admittance.

The results to be presented are for an antenna of radius c = 1 cm, a gap thickness δ of 0.1 cm and plasma parameter values typical of the E region of the ionosphere. An electron temperature of 1,500 ^{o}K will be used for the purpose of computing the vacuum sheath thickness X, which is given in units of the electron Debye length D_ℓ *. For purposes of comparison, the free-space antenna admittance is given in Fig. 1 over the frequency range 0.25 to 10 MHz, with the gap thickness a parameter on this one graph only, ranging from 10^{-1} to 10^{-3} cm. It may be seen that the conductance and susceptance are rather slowly increasing functions of the frequency and in addition, the susceptance is only slightly dependent upon the gap thickness, over this frequency range. The results of Fig. 1 will be useful in illustrating the magnitude of the perturbing influence of the plasma upon the antenna admittance.

The antenna admittance in the plasma medium is shown as a function of excitation frequency in Fig. 2 for a plasma frequency of 1.5 MHz, an electron collision frequency of 10 sec^{-1}, an electron cyclotron frequency of 1 MHz and a sheath thickness X, of 5 D_ℓ (s = 8.9988 cm) calculated for an electron temperature of 1,500 ^{o}K. The susceptance is seen to have a zero close to, or at, the upper hybrid frequency $\omega_t^2 = \omega_p^2 + \omega_h^2$ while the conductance has a rather sharp minimum there. Between the upper hybrid and plasma frequencies, the conductance and susceptance both reach a maximum, with a subsequent minimum at about the plasma frequency. Finally another larger maximum is reached between the plasma and cyclotron frequencies, with the conductance rather slowly decreasing in value as the frequency is futher decreased, while the susceptance falls off much more rapidly. The susceptance actually becomes capacitive again below approximately 0.4 MHz.

---

* $D_\ell = \sqrt{k\,T/m}\,/\omega_p$.

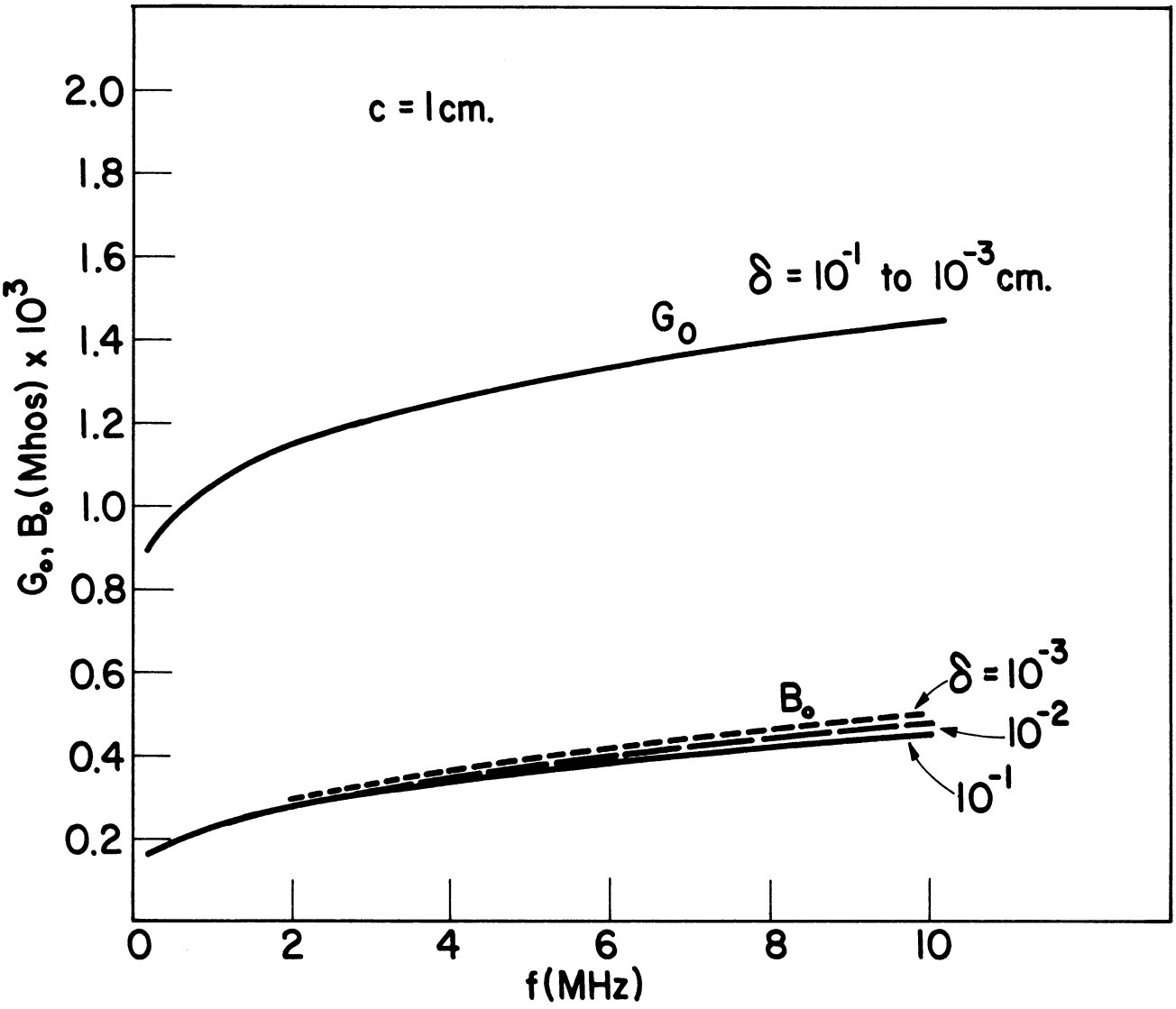

Fig. 1. The free-space infinite cylindrical antenna admittance as a function of frequency with the exciting gap thickness, δ, a parameter, and a radius, c, of 1 cm.

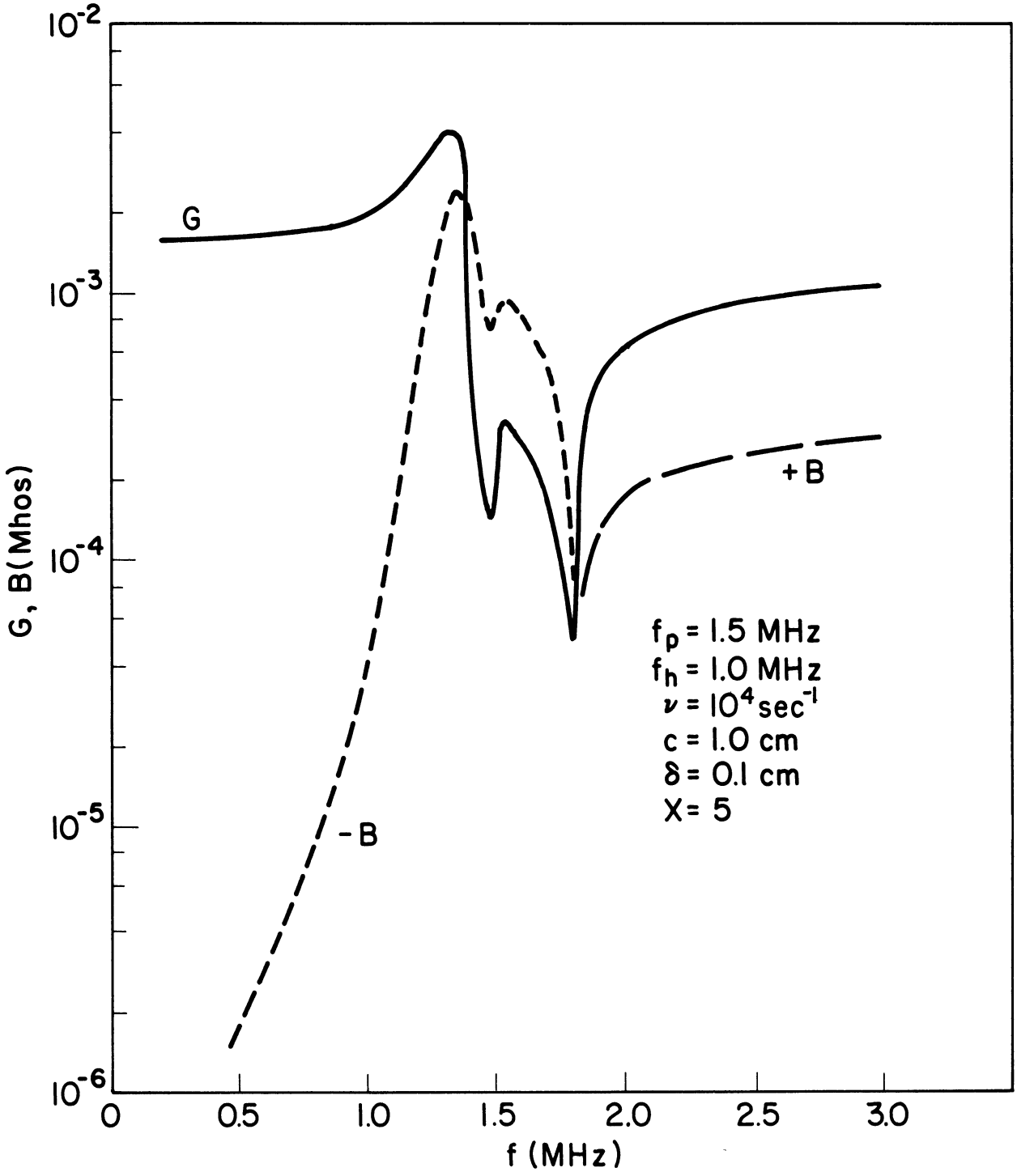

Fig. 2. The infinite antenna admittance as a function of frequency for the zero-temperature magnetoplasma with a vacuum sheath thickness, X, of $5D_\ell$, a radius of 1 cm, an electron plasma frequency of 1.5 MHz and electron cyclotron frequency of 1 MHz.

Corresponding results for the same plasma parameter values as for Fig. 2 except for zero sheath thickness are shown in Fig. 3. (The regions of the curves on this graph and those to follow where the accuracy is estimated to be no better than 10 per cent are shown by the superimposed crosses. This estimate is based on examining the variation of the integrand function and the behavior of the summed answer for (42) as the upper limit is increased in magnitude. The results are presented because while the accuracy may be less than desired, the general trend of the admittance can be exhibited.) It is apparent that the essential features of the 5 D_ℓ thick vacuum sheath results are contained in a more exaggerated form in Fig. 3. In particular, the minima in the conductance at the upper hybrid frequency and that near the plasma frequency are more pronounced, while the maximum in both susceptance and conductance has become much sharper while shifting down from just below the plasma frequency to the cyclotron frequency. Below about 0.5 MHz and above the upper hybrid frequency, the admittance for the 5 D_ℓ sheath and sheathless cases are quite similar. It is apparent from Figs. 2 and 3 that the sheath is fairly effective in decoupling the antenna from the plasma, particularly at the electron cyclotron frequency.

For purposes of comparison, the antenna admittance for the compressible, magnetic-field free plasma, with an electron temperature of 1,500 ^{o}K, is presented in Fig. 4 for $X = 5\ D_\ell$ and Fig. 5 for $X = 0$, with the other parameters the same as for Figs. 2 and 3. The susceptance zero and conductance minimum which occur for the magneto-plasma at the upper hybrid frequency are seen in the compressible magnetic-field-free plasma to occur at the plasma frequency. The strucutre of the admittance curves in Figs. 4 and 5 below the plasma frequency is not as varied as that for the previous case, but again a conductance and admittance maximum is found in this region. It is of interest to remark that the results presented in I showed that except

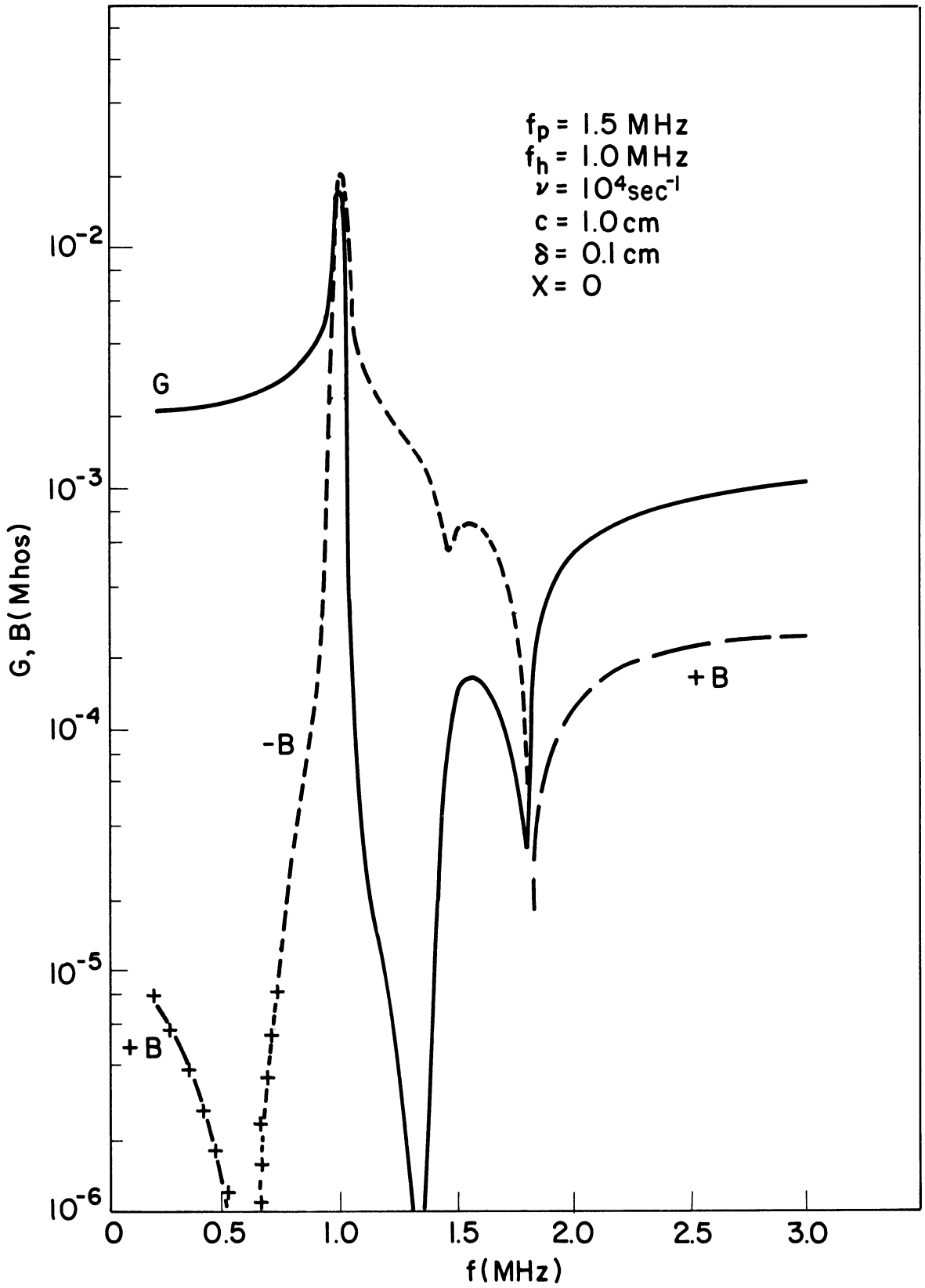

Fig. 3. The infinite antenna admittance as a function of frequency for the zero-temperature magnetoplasma with zero sheath thickness, an electron plasma frequency of 1.5 MHz and electron cyclotron frequency of 1 MHz.

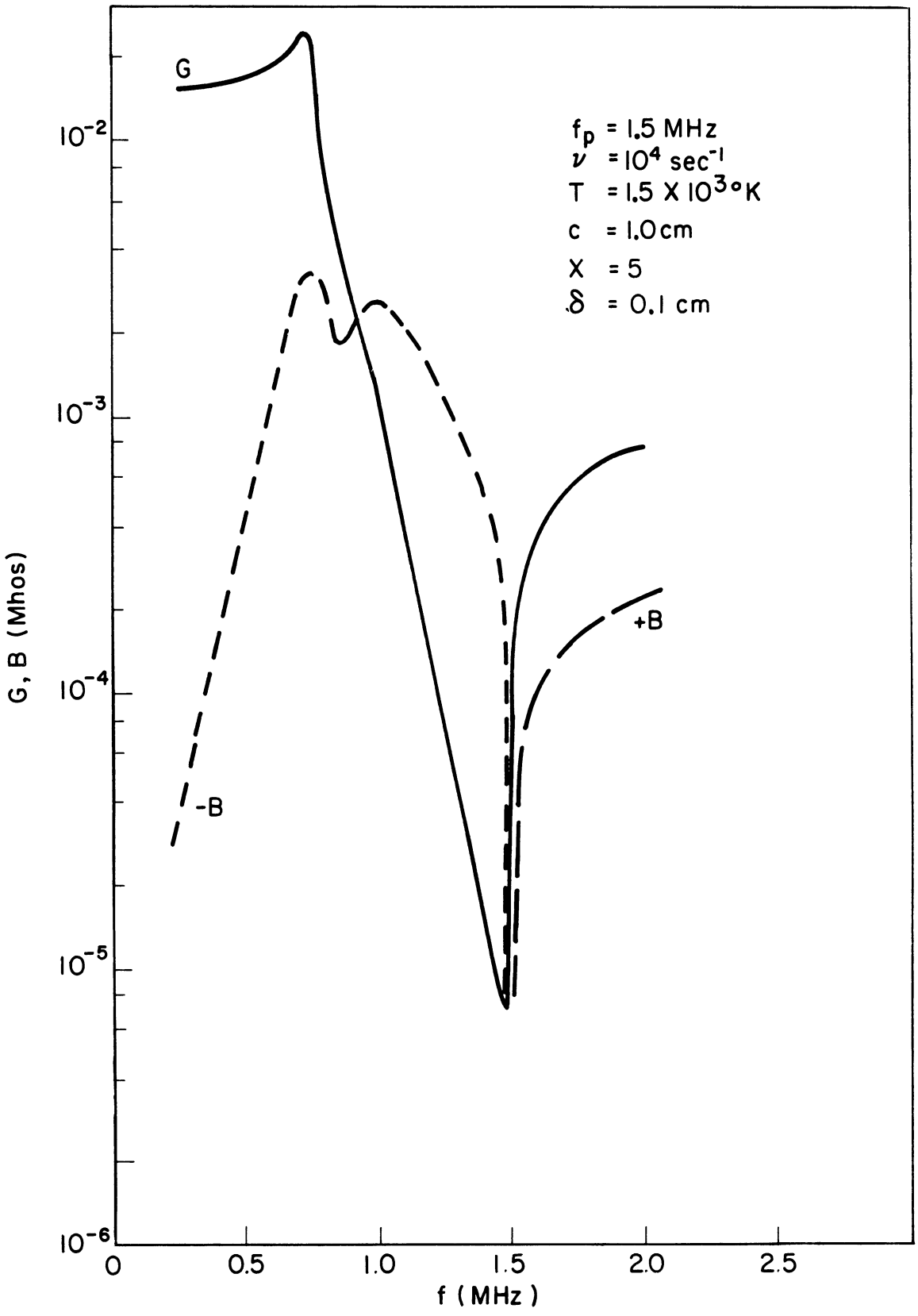

Fig. 4. The infinite antenna admittance as a function of frequency for the warm, magnetic-field-free plasma with a vacuum sheath thickness of 5 D_ℓ , and an electron plasma frequency of 1.5 MHz.

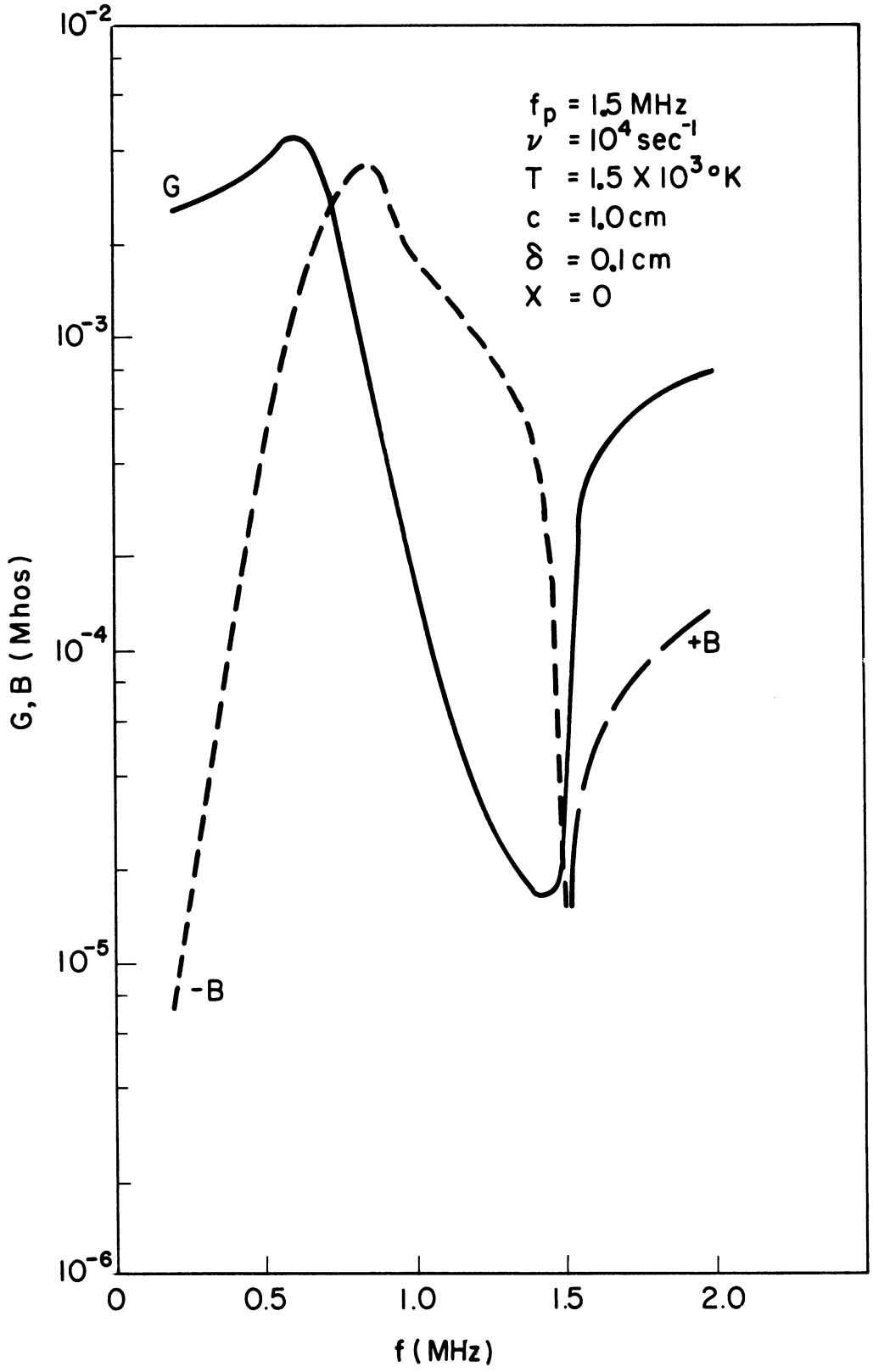

Fig. 5. The infinite antenna admittance as a function of frequency for the warm, magnetic-field-free plasma with zero sheath thickness and an electron plasma frequency of 1.5 MHz.

for the zero temperature sheathless case, an admittance maximum of this sort was found to occur below the plasma frequency. It appears that in order for such an admittance maximum to result, a sheath, magnetic field, or finite electron temperature are required.

Results corresponding to those of Figs. 2 and 3 are now given in Figs. 6 and 7, where now f_h = 1.5 MHz and f_p = 1 MHz, the other parameter values remaining the same. If we observe first the 5 D_ℓ sheath case, it may be seen that the conductance minimum at the hybrid frequency is now narrower, and that the maximum in the conductance now occurs between the cyclotron and upper hybrid frequencies. The region of inductive susceptance is also not as wide in Fig. 6 as in Fig. 2. There is a conductance minimum, not very pronounced, at the plasma frequency, while the susceptance has a sharp minimum somewhat below the plasma frequency. Above 2 MHz, the results of Figs. 2 and 6 are quite similar.

A similar comparison of Figs. 3 and 7 also shows a shifting upward of the conductance and susceptance maxima to the new location of the cyclotron frequency. Again, the region of inductive susceptance is smaller for the 1.5 MHz cyclotron frequency case, as was found for the 5 D_ℓ thick sheath. Below the cyclotron frequency, the sheathless and 5 D_ℓ thick sheath cases of Figs. 6 and 7 are quite similar, as was found previously for the 1 MHz cyclotron frequency results.

In Figs. 8 and 9 are shown the azimuthal current, $I_\varphi = 2\pi c\, K_\varphi$, calculated also at $z = \delta/2$, for the 5 D_ℓ and zero sheath thickness cases respectively and the same plasma parameters as Figs. 6 and 7. The azimuthal current is seen to be most strongly excited in the vicinity of the upper hybrid frequency for the 5 D_ℓ thick case, and except in this area is less than 10^{-2} of the axial current. For the sheathless case, the aximuthal current is largest at the cyclotron frequency and is larger by comparison with the axial current

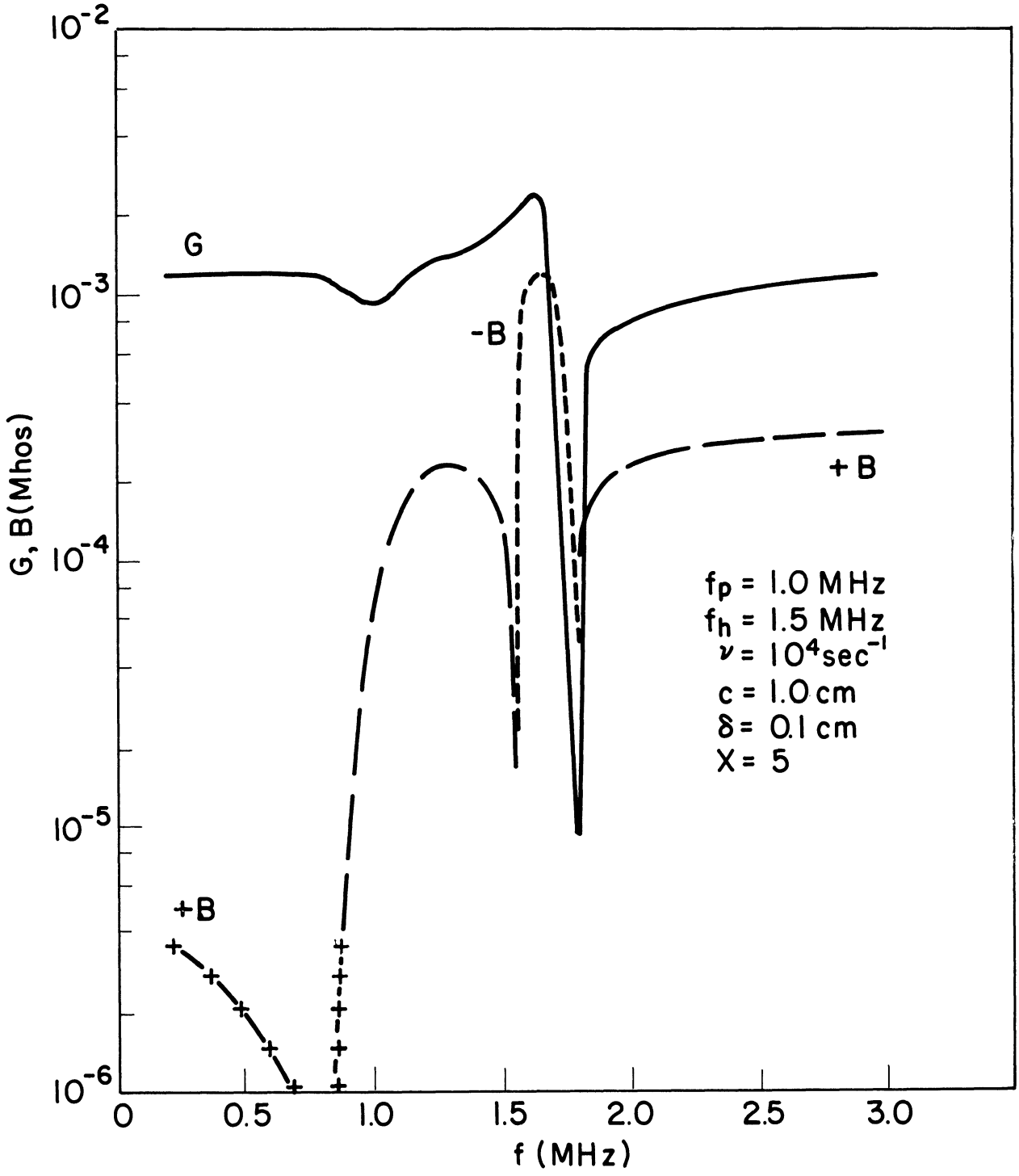

Fig. 6. The infinite antenna admittance as a function of frequency for the zero temperature magnetoplasma with a vacuum sheath thickness of 5 D_ℓ , an electron plasma frequency of 1 MHz and an electron cyclotron frequency of 1.5 MHz.

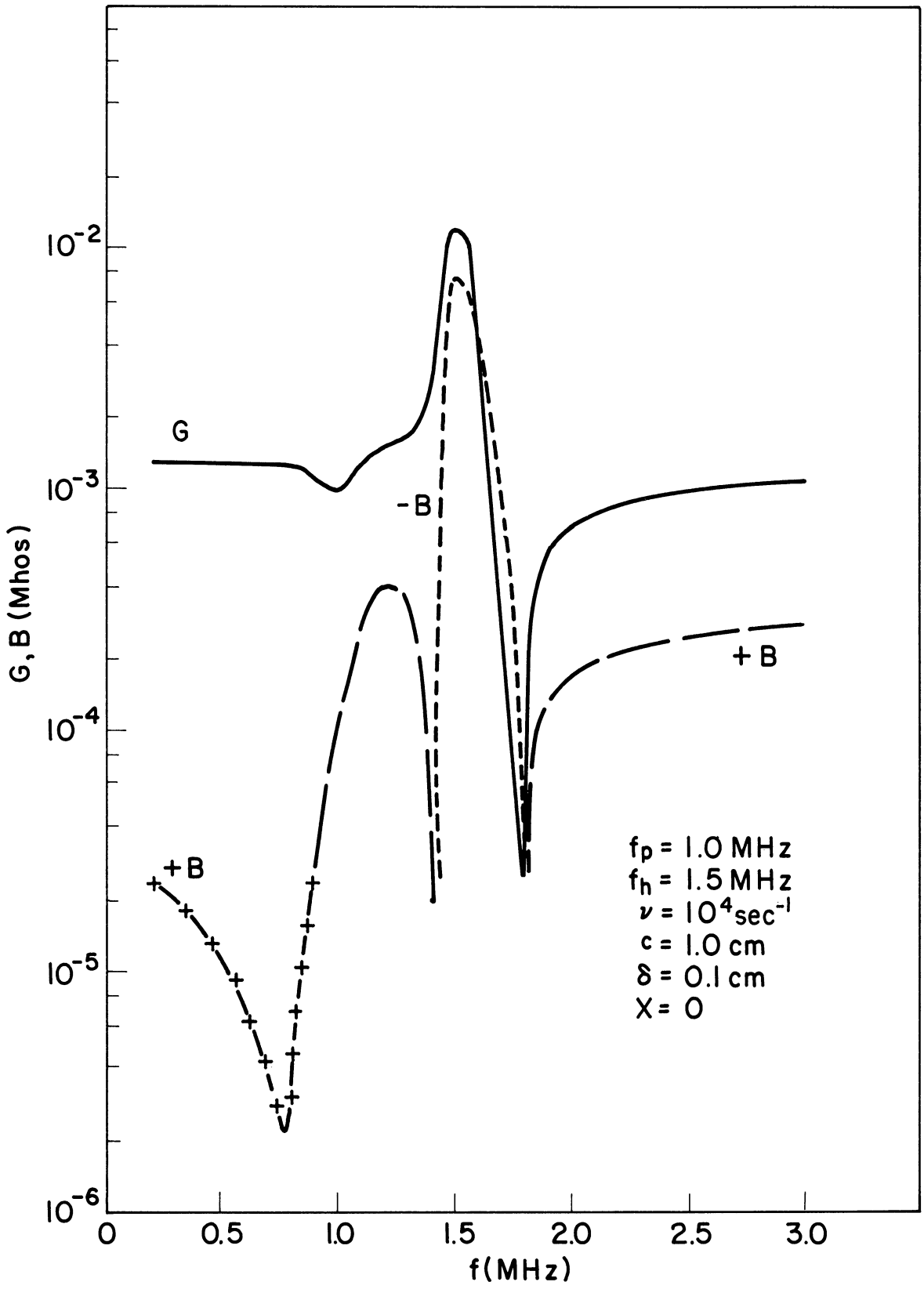

Fig. 7. The infinite antenna admittance as a function of frequency for the zero temperature magnetoplasma with zero sheath thickness, an electron plasma frequency of 1 MHz and an electron cyclotron frequency of 1.5 MHz.

than the situation for the 5 D_ℓ thick sheath. The sheathless current is seen to exhibit the basic features of the 5 D_ℓ thick sheath results, as was the case for the z-component of current in the preceding graphs. Values are not given for $f < 0.9$ MHz in Fig. 9 because of uncertainty in the results. It was mentioned that only $I_z(\mathcal{O}/2, \omega)$ was subjected to the convergence test involved in the numerical integration of the integral (42) and (43) because our primary concern has been to obtain the antenna admittance. Consequently, the numerical accuracy of I_φ cannot be specified; however, values are given in Figs. 8 and 9 only where the convergence of I_φ appears to be reliable.

The azimuthal current arises because the axial magnetic field causes the antenna to excite a wave with a z-component of magnetic field, a wave which is not excited when the static magnetic field is zero. Consequently, it is not unexpected that the azimuthal current is maximum near the electron cyclotron frequency. The total surface current on the antenna which results from adding the z and φ components is helical in nature.

As the last graph of this series we present in Fig. 10a the antenna admittance as a function of plasma frequency for a fixed excitation frequency of 1.0 MHz and a cyclotron frequency of 1.47 MHz, with the other parameter values as in the preceding graphs. These values of exciting frequency and cyclotron frequency were chosen to conform to some experimental data of Stone, Weber and Alexander (1966) obtained from a rocket-borne antenna in the ionosphere.

The conductance is seen to be fairly constant for $f_p < f$ but increases almost exponentially with increasing f_p beyond this point. The susceptance is capacitive for $f_p < 1.25$ MHz but becomes inductive for larger f_p. The calculated values of the susceptance are not very reliable for $f_p \approx 1.5$ MHz because of computational problems related to overflow. This consideration is important in this range of f_p because the susceptance is essentially obtained

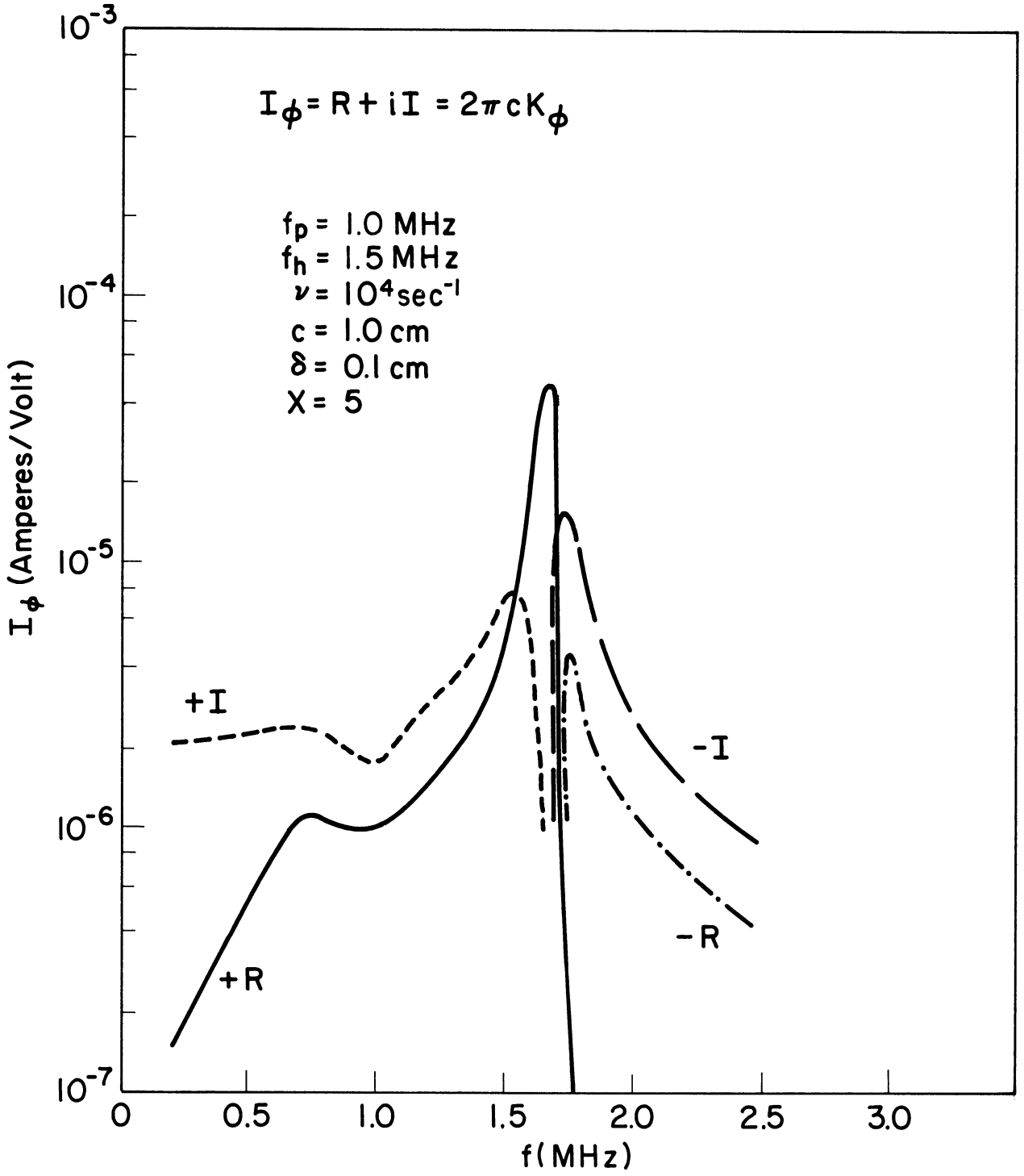

Fig. 8. The azimuthal current component as a function of frequency for the zero-temperature magnetoplasma with a vacuum sheath thickness of 5 D_ℓ , an electron plasma frequency of 1 MHz and an electron cyclotron frequency of 1.5 MHz.

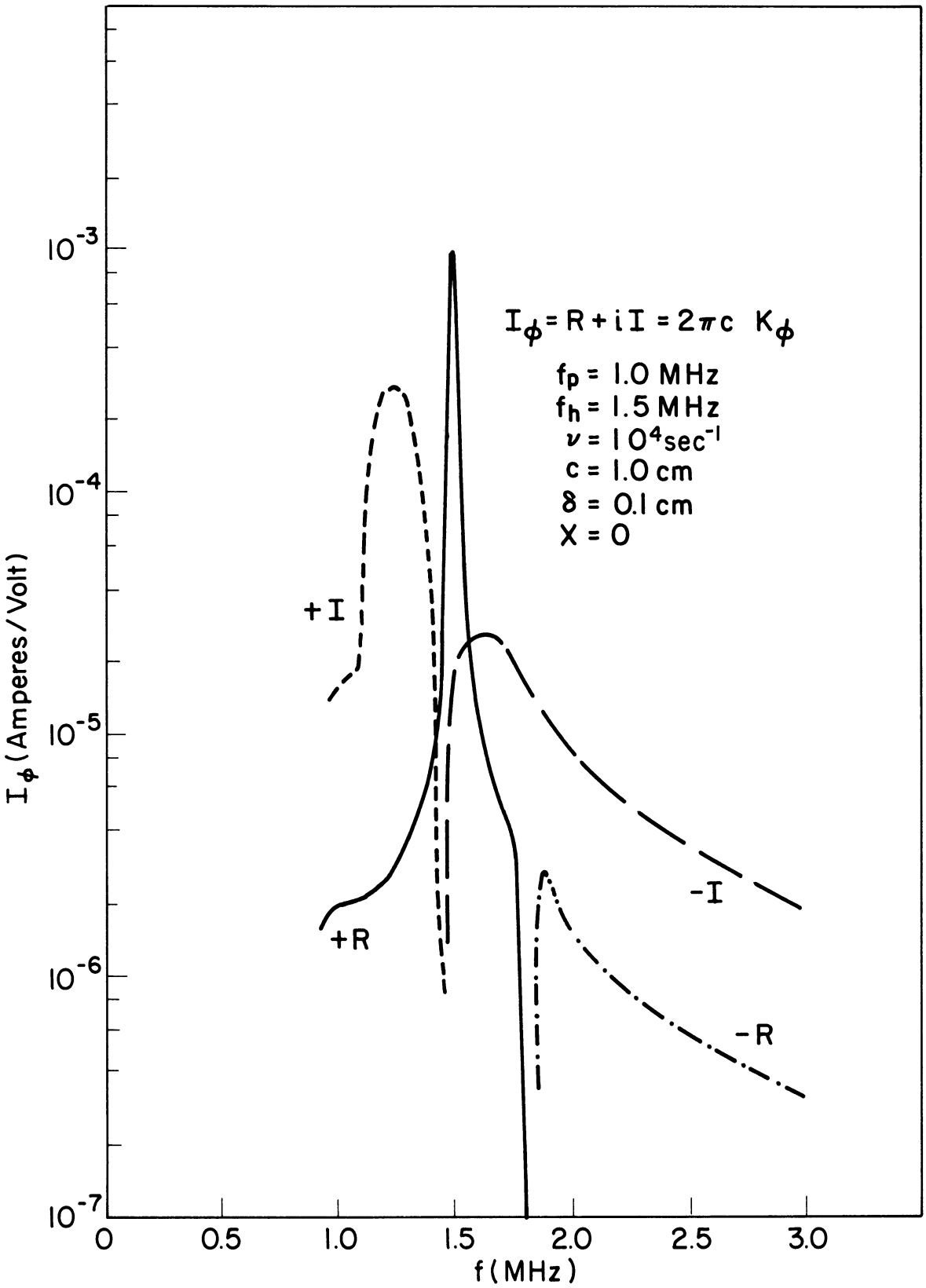

Fig. 9. The azimuthal current component as a function of frequency for the zero-temperature magnetoplasma with zero sheath thickness, an electron plasma frequency of 1 MHz and an electron cyclotron frequency of 1.5 MHz.

as the difference of two numbers large compared with the final answer. Consequently the error resulting from the overflow termination before the truncation error is acceptably small is most important here. For f_p values greater than 2 MHz this problem is not as serious.

It is interesting to compare the results of Fig. 10a with the experimental measurements of Stone et. al. mentioned above (given in their Fig. 4 and shown in Fig. 10b), which are plotted as measured reactance and resistance divided by the free space impedance of the antenna. The admittance values of Fig. 10a may be used to obtain impedance values (also shown on Fig. 10a), of which the resistive part exhibits a slight peaking and then a decreasing trend with increasing f_p, as do the measured resistances. The measured reactance however, does not change from capacitive to inductive as does the calculated value for the infinite antenna. The calculated results are for a static magnetic field parallel to the infinite antenna, while the expremental results are for the situation where the antenna is almost perpendicular to the field, so that some of the difference between theory and experiment may be due to this factor. In addition, the calculated results are for the sheathless case, and it has been found that a sheath may somewhat reduce the region of inductive susceptance. And finally, the calculations are for the infinite dipole and a comparison with measured results, particularly the reactance whose sign is dependent upon the antenna length, must bear this in mind. On the whole, the calculated and measured impedances show a similar qualitative behavior as a function of plasma frequency.

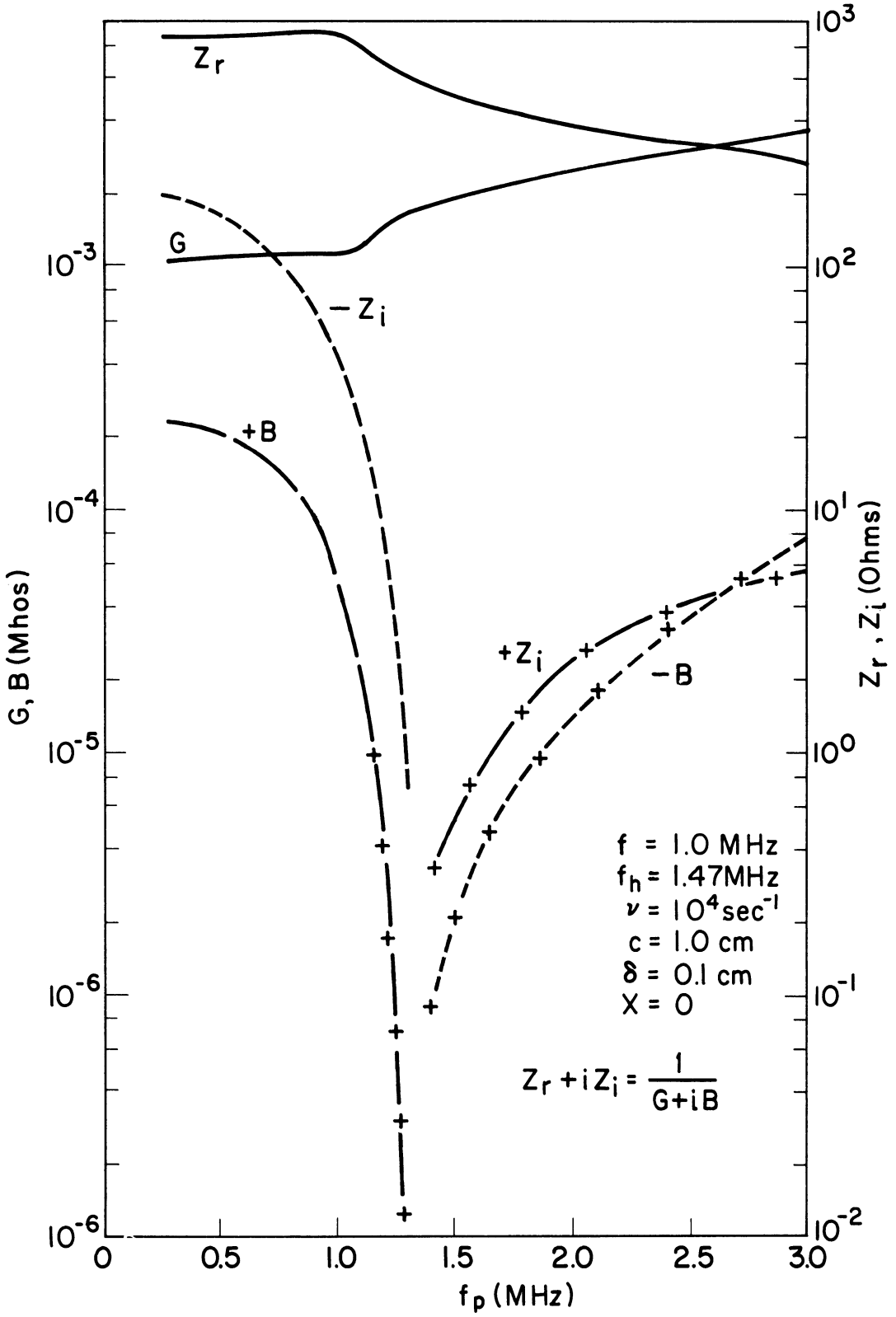

Fig. 10a. The infinite antenna admittance and impedance as a function of electron plasma frequency for the zero-temperature magnetoplasma with zero sheath thickness, an electron cyclotron frequency of 1.47 MHz and excitation frequency of 1 MHz.

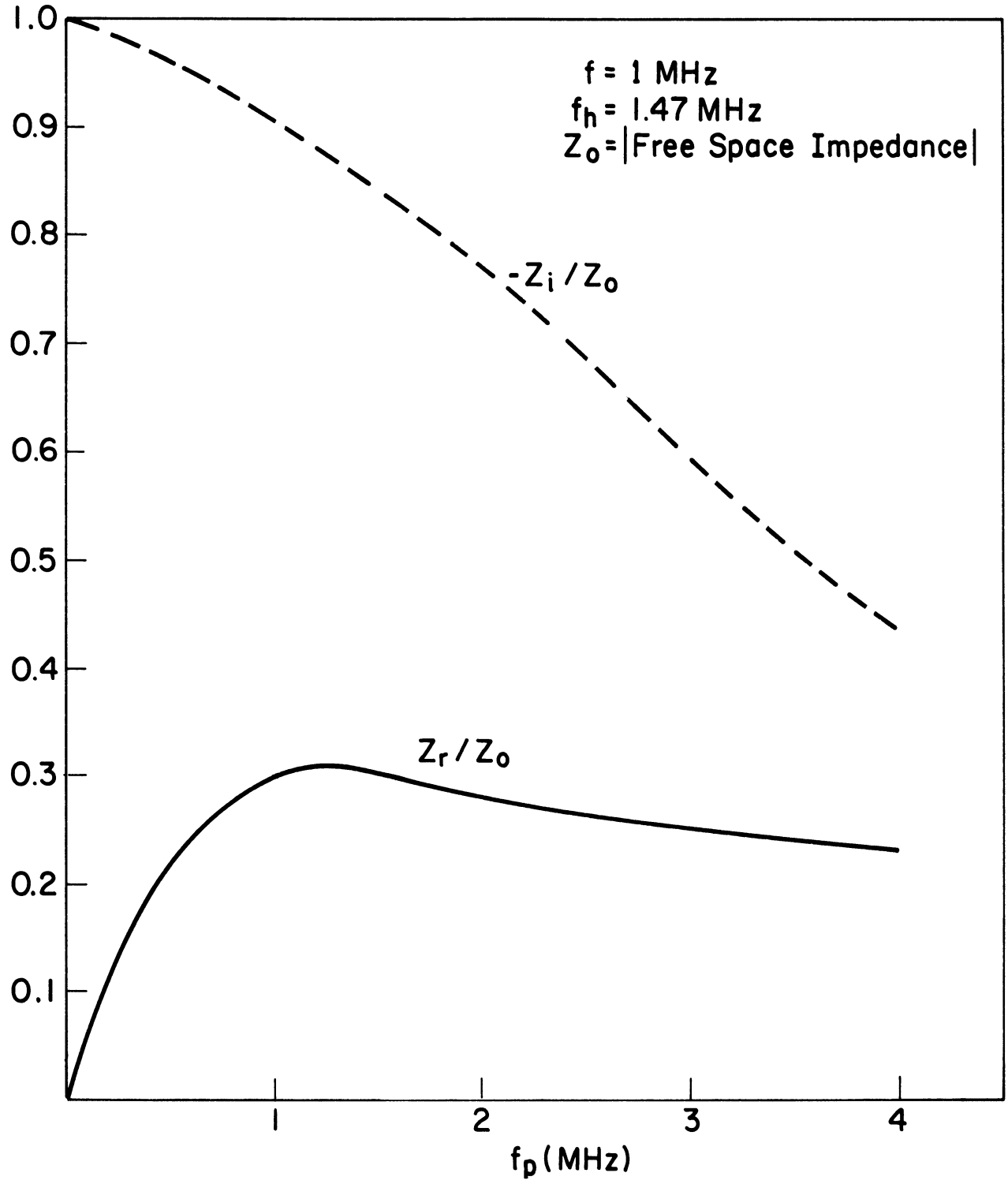

Fig. 10b. The experimental results of Stone, Weber and Alexander (1966) as a function of electron plasma frequency and excitation frequency of 1 MHz.

III. 2. Comparison of Finite and Infinite Antenna Results:

We now present for purposes of comparison some admittance curves for a finite length dipole antenna of half-length h equal to 3.048m(10ft.) immersed in a zero-temperature magnetoplasma with a parallel magnetic field calculated from an expression derived by Balmain (1964). The dipole radius is 1 cm, the same as that of the infinite antenna just discussed. The admittance curves are shown in Fig. 11 for f_h = 1. MHz and f_p = 1.5 MHz, and in Fig. 12 for f_h = 1.5 MHz and f_p = 1 MHz, and with ν = 10 sec^{-1}, the value previously used.

A comparison of Fig. 11 with the corresponding sheathless case for the infinite antenna of Fig. 3 shows that the finite antenna admittance is qualitatively very similar to that of the infinite antenna for the frequency range encompassing the electron cyclotron frequency and upper hybrid frequency . In both cases the structure of the curves is similar, though their magnitudes are different. Each of the antennas has an admittance maximum at the electron cyclotron frequency, while the conductance of each exhibits a rather well pronounced maxima and the susceptance a less sharp discontinuity in slope near the electron plasma frequency.

The principal differences between Figs. 3 and 11 is the area below the electron cyclotron frequency of 1 MHz, where the infinite antenna susceptance remains inductive until the frequency becomes less than 0.6 MHz, in contrast to the finite antenna susceptance which becomes inductive immediately below f_h. In addition the finite antenna conductance decreases rather sharply with decreasing frequency whereas the infinite antenna conductance rate of decrease is much less. Above the upper hybrid frequency, the finite and infinite antenna susceptances are similar. The conductances however differ in this range by orders of magnitude, while also the finite antenna conductance has no minimum as does the infinite

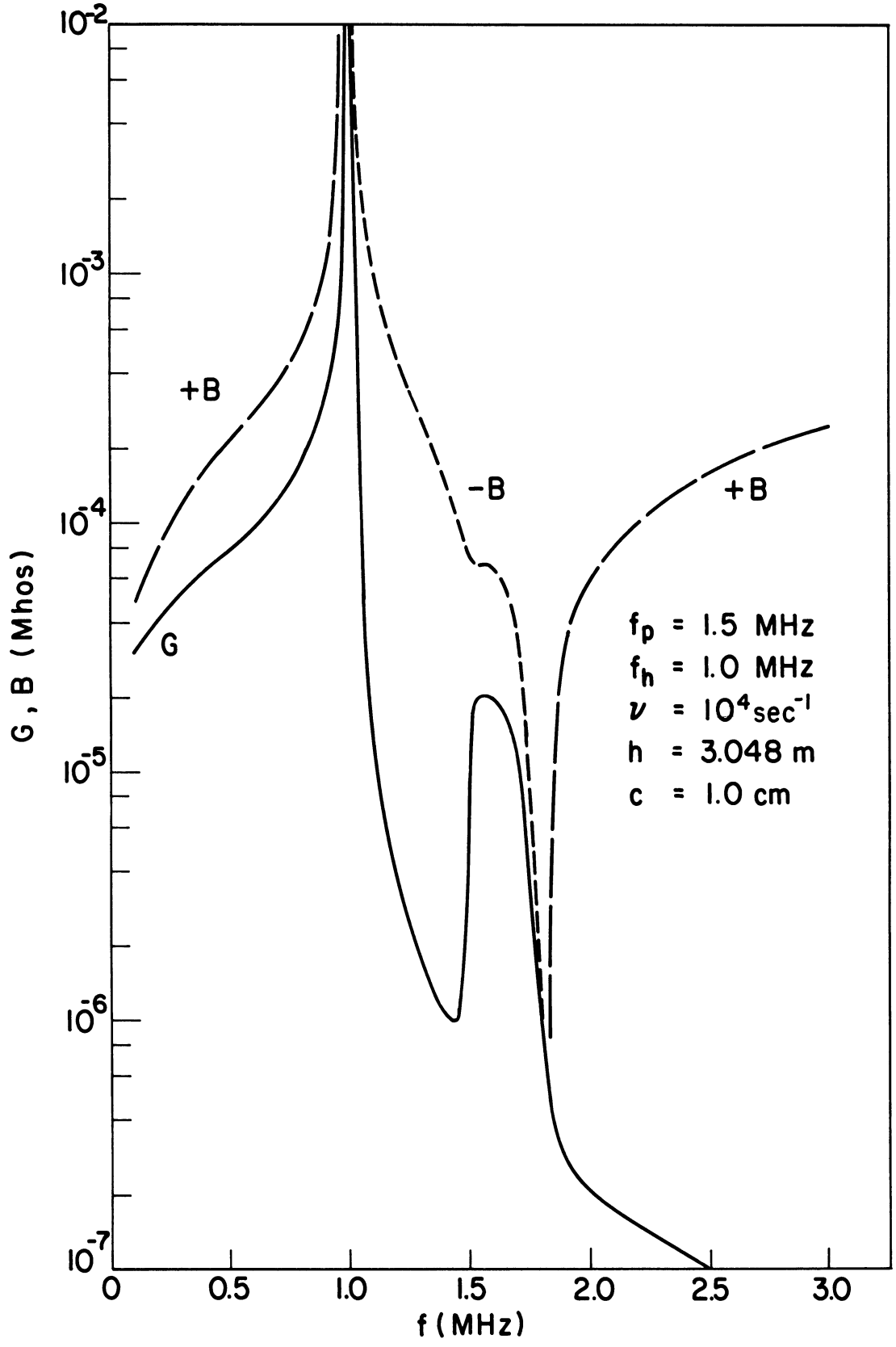

Fig. 11. The finite antenna admittance as a function of frequency for the zero-temperature magnetoplasma with an electron plasma frequency of 1.5 MHz and electron cyclotron frequency of 1 MHz from the theory of Balmain (1964).

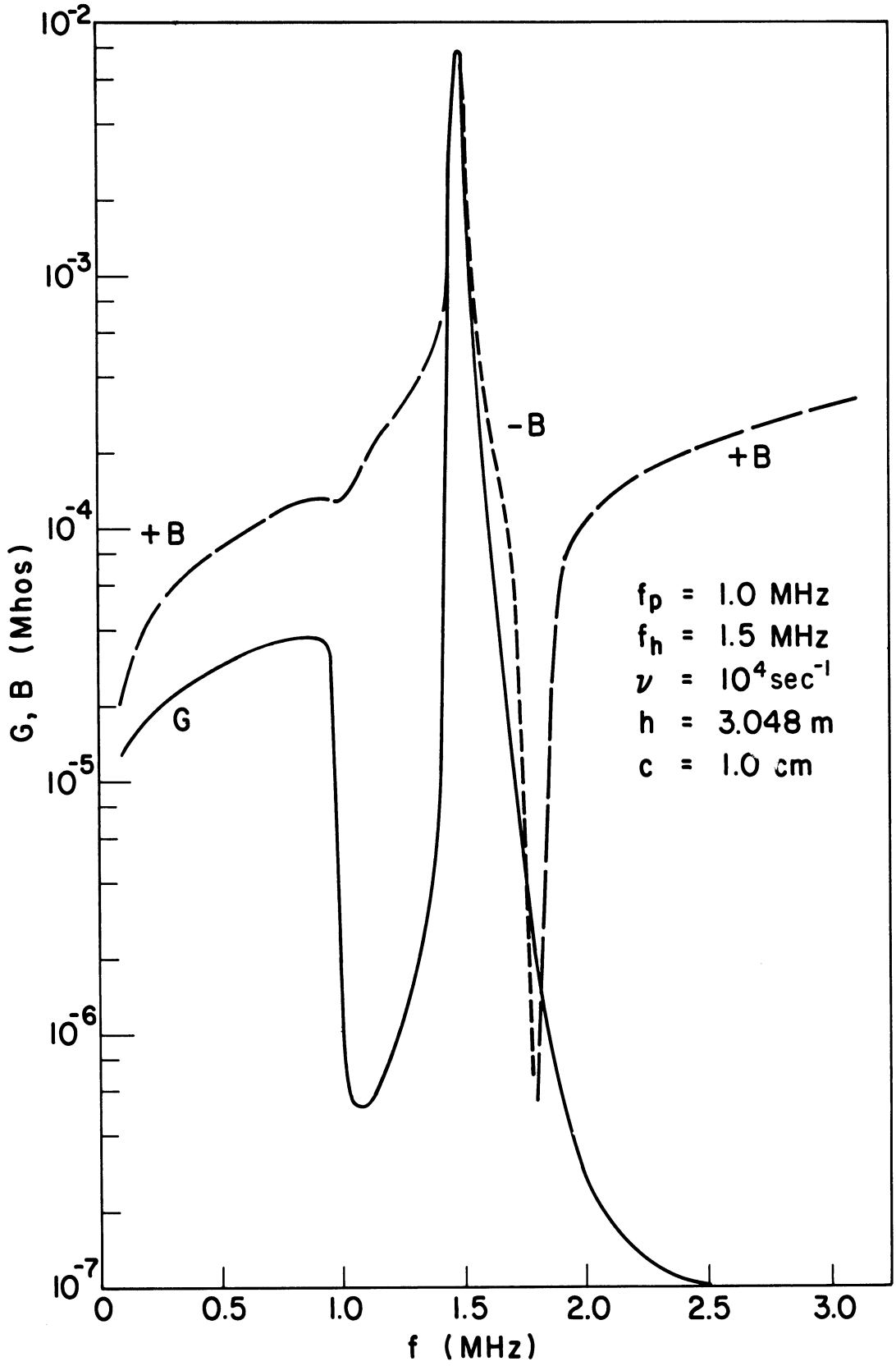

Fig. 12. The finite antenna admittance as a function of frequency for the zero-temperature magnetoplasma with an electron plasma frequency of 1 MHz and electron cyclotron frequency of 1.5 MHz from the theory of Balmain (1964).

antenna, at the upper hybrid frequency. This difference between the finite and infinite antenna conductances near the upper hybrid frequency may be explained by taking into account the difference between their free-space admittances and the near-field antenna behavior; a discussion is given in I.

If Figs. 7 and 12 are now examined where the results for $f_p < f_h$, are presented the infinite and finite antenna admittances may be seen to compare with each other in somewhat the same fashion as the case for $f_p > f_h$. The conductance and susceptance are seen to have a maximum at the electron cyclotron frequency. A rather shallow minimum in the infinite antenna conductance and a much deeper minimum in the finite antenna conductance are seen to occur near the plasma frequency, while the converse behavior is observed in the susceptances. Again, the finite antenna susceptance is inductive between the upper hybrid and electron cyclotron frequencies, while the infinite antenna inductive susceptance region extends to a slightly lower frequency. Above the upper hybrid frequency and below the plasma frequency, there is the greatest difference between the admittances of the infinite and finite antennas, as in the case for $f_p > f_h$.

It is of significance and interest to note that both the finite antenna admittance results, presented in Figs. 11 and 12, and the infinite antenna results previously given, exhibit a discontinuity in slope or a minimum in the admittance, at the electron plasma frequency, a feature exhibited by the experimental data of Heikkila et al (1966), obtained from a rocket-borne antenna in the ionosphere. This characteristic of the experimental admittance results was used by Heikkila et al to obtain electron density values, although their application of this technique was apparently empirical, not having been predicted by

any theory and instead showing up unexpectedly in their data. The theoretical results obtained here would appear to provide some means for explaining the experimental data and provide a firmer basis for further exploiting this feature of the antenna admittance as an additional technique for measuring ionospheric electron densities. It is of interest to mention that in addition, the experimental results of Heikkila et al (1966) show an admittance maximum slightly above the electron cyclotron frequency. In view of the calculated admittance values presented here, this location of the admittance maximum would seem to indicate the presence of a sheath, which the calculations have shown, would shift such an admittance maximum upward from the cyclotron frequency.

IV. Summary and Conclusions.

This investigation has been concerned with finding the admittance of an infinite, cylindrical antenna which is excited at a circumferential gap of finite thickness and immersed in a zero-temperature, lossy, anisotropic plasma with its axis parallel to the static magnetic field. The antenna admittance has been obtained numerically over a frequency range encompassing the electron plasma and cyclotron frequencies and the upper hybrid frequency for plasma parameter values typical of the E-region of the ionosphere. A vacuum sheath model and inhomogeneous sheath model were considered in the analysis, but only the vacuum sheath model was used in obtaining the numerical results. In addition to the admittance, which involves finding the axial antenna current, some results were given for the azimuthal antenna current. Finally a comparison of the infinite antenna results were made with admittance values obtained from a finite antenna model due to Balmain.

The infinite antenna admittance results presented show that the vacuum sheath tends to decouple the antenna from the plasma, particularly at the electron cyclotron frequency, and more generally has the effect of reducing the magnitude of the admittance variations in the frequency range encompassing the upper hybrid, electron cyclotron and electron plasma frequencies, compared with the sheathless case. For frequencies outside this range, the sheath has relatively little effect on the admittance, especially above the upper hybrid frequency. The sheath in addition appears to have its greatest influence when the electron cyclotron frequency is less than the electron plasma frequency.

The antenna susceptance is capacitive above the upper hybrid frequency, becoming inductive below this frequency. The susceptance may again become capacitive when the frequency is less than the electron cyclotron frequency, with the location of the susceptance zeros appearing to have no relation to the

plasma frequency. The electron plasma frequency appears to be related to admittance minima which occur near it, but does not generally appear to give rise to as marked variations in antenna admittance as the electron cyclotron and upper hybrid frequencies. The conductance is, broadly speaking, larger above the electron plasma frequency and less below it for the 5-D_ℓ thick sheath as compared with the sheathless case. Similarly speaking, the susceptance is more capacitive for frequencies above the electron cyclotron frequency and more inductive below it for the 5-D_ℓ sheath compared with the sheathless case.

A comparison of the zero-temperature magnetoplasma admittances with corresponding results for the magnetic-field-free warm plasma with a temperature of 1500°K shows that the admittance minimum which occurs at the upper hybrid frequency in the former case is shifted to the electron plasma frequency in the latter. The results for the two plasma models above these respective frequencies are quite similar, while for frequencies less than these the admittances are generally quite different. It is interesting to note however, that an admittance maximum is found to occur below the upper hybrid or electron plasma frequency for the respective plasma models mentioned above, but which is not present when the magnetic field, sheath thickness and temperature are all zero.

Some admittance results obtained for a finite antenna oriented parallel to the static magnetic field and using the same plasma parameter values as for the infinite antenna calculations reveals that while their admittance magnitudes are quite different, there is a qualitative similarity in the frequency variation. A similar result was previously found in I for the zero-temperature, magnetic-field-free plasma. Consequently, it would appear the infinite antenna results may be useful in at least qualitatively determining the effects on the admittance of a finite antenna of varying the various plasma parameters, at least for the sheathless case. While this may not appear to be an advantage in the situation mentioned

since closed-form expressions are already available for the finite antenna, that is not the case for the non-zero temperature plasma, with or without a magnetic field. Thus the infinite antenna analysis may serve a very useful purpose for the latter case. In addition, the infinite antenna analysis may also include a sheath, a feature not presently available in the finite antenna approach, which as has been seen, may have a considerable influence on the antenna admittance. Some caution must be exercised here however, since the sheath can support surface waves which may to some extent nullify the correspondence between the infinite antenna admittance and the results for a similarly sheathed, finite antenna.

The results thus far obtained in I and the present study have provided some basis for comparison with, and interpretation of, experimental measurements of antenna admittance in an ionized medium. It appears that further effort in the direction of extending the analysis to the more general case of the compressible magnetoplasma is indicated, particularly since some experimental swept-frequency measurements of the admittance of a rocket-borne antenna are planned. The use of the inhomogeneous sheath model also appears to be to worthwhile carrying out in order to gain some insight into the relative validity of the vacuum sheath and sheathless models. Finally, it appears that it may be useful to investigate the possibility of using the infinite antenna current as a means of obtaining a solution to the finite antenna. One analysis that uses this approach is due to Chen and Keller (1962).

Appendix A: Examination of the Singularities in the Current Integral

We want to establish that while the two components of $I_z = I_{zo} + \Delta I_z$ contain non-integrable singularities at $\beta = K_{Eo}$, their sum does not, so that Eq. (42) may be integrated along the real β -axis, so long as the electron collision frequency is non-zero. A discussion of the singularities of I_{zo} is given in Appendix A of I, where it is shown that the real part of the current, I_{or}, is proportional to

$$I_{or} \propto \int \frac{dx}{x(\ln x)^2} = -\frac{1}{\ln (x)}$$

in the vicinity of $\beta = K_{Eo}$, where

$$x = \left[2 (K_{Eo} - \beta) / K_{Eo}\right]^{\frac{1}{2}} K_{Eo}\, c$$

and I_{or} is thus integrable at $\beta = K_{Eo}$. The imaginary part of I_{zo}, denoted by I_{oi}, is similarly proportional to

$$I_{oi} \propto \int \frac{dx}{x \ln x} = \ln (\ln x)$$

at $\beta = K_{Eo}$ and is thus non-integrable there.

This being the case, it is then necessary to show that ΔI_z has the same behavior as I_{zo} in the vicinity of $\beta = K_{Eo}$, but is of opposite sign, so that the integrand of Eq. (42) will be a proper one. If we examine Eqs. (37) and (38) using the small argument approximations for the cylindrical functions of argument proportional to λ_{Eo}, it may be shown from the second and third lines of Eq. (37) that

$$\bar{A}_1, \bar{A}_2 \longrightarrow \lambda_{Eo}^2 \bar{A}_e I$$

$$\lim \beta \longrightarrow K_{Eo}$$

Consequently, upon using lines (1) and (4) of Eq. (37), it follows that

$$\bar{A}_m^I \longrightarrow \frac{K_{Eo}}{2\lambda_{Eo}^2}$$

$$\lim \beta \to K_{Eo}$$

From Eq. (35a) we then find that

$$\bar{A}_m^R \longrightarrow \frac{K_{Eo}}{2\lambda_{Eo}^2}$$

$$\lim \beta \to K_{Eo}$$

Thus that part of the integrand of Eq. (42) in the square brackets goes as

$$\left[\ \right] = \left[\frac{K_{Eo}}{\lambda_{Eo}} H_o^{(2)'}(\lambda_{Eo} c) + \frac{4i}{\pi c} \bar{A}_m^R\right]$$

$$\longrightarrow \left[-\frac{2i\, K_{Eo}}{\lambda_{Eo}^2\, \pi c} + \frac{2i\, K_{Eo}}{\lambda_{Eo}^2\, \pi c}\right]$$

$$\lim \beta \to K_{Eo}$$

so that the non-integrable parts of the integral do indeed cancel. That is not to say however that the integrand of Eq. (42) becomes zero at $\beta = K_{Eo}$, since we have considered here only the dominant terms. That part of $\bar{A}_m^R$ which has been neglected compared with the dominant term does contribute to the integral at $\beta = K_{Eo}$. Note that terms which vary as λ_{Eo}^p in the bracket of Eq. (42), where $p > -2$ will be integrable at the singularity and contribute to the current integral there.

References

Balmain, K. G. (1964), The impedance of a short dipole antenna in a magnetoplasma, IEEE Trans. AP-12, No. 5, 605-617.

Chen, Y. and J. B. Keller (1962), Current on and input impedance of a cylindrical antenna, J. or Res. NBS, Section D, 66D, No. 1, 15-21.

Duncan, R. H. (1962), Theory of the infinite cylindrical antenna including the feedpoint singularity in antenna current, J. of Res. NBS 66D, No. 2, 181-188.

Einarsson, Olov (1966), A comparison between tube shaped and solid cylinder antenna, IEEE Trans. AP-14, No. 1, 31-37.

Fante, R. L. (1966), On the admittance of the infinite cylindrical antenna, Radio Sci. 1, No. 9, 1041-1044.

Heikkila, W. J., J. A. Fejer, J. Hughill and W. Calvert (1966), Comparison of ionospheric probe techniques, Southwest Center for Advances Studies, Report DASS-66-5.

Miller, E. K. (1966a), Excitation of surface currents on a plasma-immersed cylinder by electromagnetic and electrokinetic waves, U. or Mich. Scientific Report 05627-4-S.

Miller, E. K. (1966b), Surface current excitation on an inhomogeneously-sheathed, plasma immersed cylinder by electromagnetic and electrokinetic waves, U. of Mich. Scientific Report 05627-5-S.

Miller, E. K. (1967a), The admittance of the infinite cylindrical antenna in a lossy, isotropic, compressible plasma, U. of Michigan Scientific Report 05627-10-S.

Miller, E. K. (1967b), Admittance dependence of the infinite cylindrical antenna upon exciting gap thickness, to be published in Radio Science.

Seshadri, S. R. and T. T. Wu, Radiation condition for a magneto plasma medium - I, Applied Res. Lab., Sylvania Elect. Systems Res. Report 502.

Stone, R. G., R. R. Weber and J. K. Alexander (1966), "Measurement of Antenna impedance in the ionosphere - I. Observing frequency below the electron gyro frequency", Planet. Space Sci. Vol 14, 631-639.